

Characterization of innexin gene expression and functional roles of gap-junctional communication in planarian regeneration

Taisaku Nogi, Michael Levin*

Department of Cytokine Biology, The Forsyth Institute, 140 The Fenway, Boston, MA 02115, USA

Department of Oral and Developmental Biology, Harvard School of Dental Medicine, 140 The Fenway, Boston, MA 02115, USA

Received for publication 17 January 2005, revised 20 August 2005, accepted 1 September 2005

Available online 21 October 2005

Abstract

Planaria possess remarkable powers of regeneration. After bisection, one blastema regenerates a head, while the other forms a tail. The ability of previously-adjacent cells to adopt radically different fates could be due to long-range signaling allowing determination of position relative to, and the identity of, remaining tissue. However, this process is not understood at the molecular level. Following the hypothesis that gap-junctional communication (GJC) may underlie this signaling, we cloned and characterized the expression of the Innexin gene family during planarian regeneration. Planarian innexins fall into 3 groups according to both sequence and expression. The concordance between expression-based and phylogenetic grouping suggests diversification of 3 ancestral innexin genes into the large family of planarian innexins. Innexin expression was detected throughout the animal, as well as specifically in regeneration blastemas, consistent with a role in long-range signaling relevant to specification of blastema positional identity. Exposure to a GJC-blocking reagent which does not distinguish among gap junctions composed of different Innexin proteins (is not subject to compensation or redundancy) often resulted in bipolar (2-headed) animals. Taken together, the expression data and the respecification of the posterior blastema to an anteriorized fate by GJC loss-of-function suggest that innexin-based GJC mediates instructive signaling during regeneration.

© 2005 Elsevier Inc. All rights reserved.

Keywords: Planaria; Regeneration; Innexins; Gap-junctional communication; Patterning

Introduction

The restoration of body structures following injury requires an initiation of growth and an imposition of correct morphology upon the regenerating tissue. Understanding this process is crucial both for the basic biology of pattern formation as well as for developing novel biomedical approaches. Planaria possess remarkable powers of regeneration (Morgan, 1901), and are now becoming an important model system for understanding the molecular mechanisms which underlie this phenomenon (Alvarado and Newmark, 1998; Newmark and Alvarado, 2002; Reddien and Alvarado, 2004). Regeneration is fairly rapid (complete after 7 days) and is dependent upon a population of stem cells (neoblasts). After bisection across the

main body axis, the anterior blastema will regenerate a head while the posterior blastema will regenerate a tail. Importantly, these radically different fates are adopted by cells that were adjacent neighbors before the (arbitrarily placed) cut. Thus, it is unlikely that purely local mechanisms can explain the specification of identity along the anterior–posterior (AP) axis of the blastemas.

In contrast, models can be formulated where the blastema's AP identity is dependent upon long-range signaling which allows cells to ascertain their position relative to, and the identity of, remaining tissue (Kobayashi et al., 1999a,b; Nogi and Watanabe, 2001). For example, a blastema which receives information to the effect that the other end of the animal contains a tail can safely assume it must form a head. However, this process is not understood at the molecular level. To lay the ground for establishment of testable, mechanistic models of this process, we focused on one candidate system for establishing long-range signaling during axial patterning: gap-junctional communication (GJC). A similar proposal has been made for

* Corresponding author. Department of Cytokine Biology, The Forsyth Institute, 140 The Fenway, Boston, MA 02115, USA. Fax: +1 617 892 8597.

E-mail address: mlevin@forsyth.org (M. Levin).

control of regeneration polarity in *Hydra* (Fraser et al., 1987; Wakeford, 1979).

Gap-junctions permit the direct transfer of small (<1 kDa) signaling molecules between adjacent cells (Falk, 2000; Goodenough et al., 1996). This forms an alternative to the better-understood secreted messenger/receptor systems that function in morphogenesis (Falk, 2000; Goodenough et al., 1996; Krutovskikh and Yamasaki, 2000). GJC is now known to be a general mechanism for achieving rapid syncytial communication within cell groups, including the spread of electric waves in cardiac tissue (Kimura et al., 1995; Severs, 1999) and the brain (Budd and Lipton, 1998), and the transmission of signals through gland cells to synchronize hormonal action and secretion (Levin and Mercola, 2000; Meda, 1996). Other aspects of cellular control via GJC have been revealed by the inverse functional relationship between tumor growth and GJC (Krutovskikh and Yamasaki, 1997; Omori et al., 1998; Omori et al., 2001).

An especially important role for gap-junctional communication is in the control of patterning (Levin, 2001; Lo, 1996; Warner, 1999). In vertebrate model systems, gap-junction-mediated signaling events have been implicated in heart (Ewart et al., 1997; Lo et al., 1999) and limb (Allen et al., 1990; Coelho and Kosher, 1991; Makarenkova et al., 1997; Makarenkova and Patel, 1999) development. Interestingly, in chick and frog embryos, GJC-mediated long-range signal exchange between the left and right sides is required for the early steps of left–right patterning (Levin and Mercola, 1998; Levin and Mercola, 1999). These data suggest the possibility that GJC may underlie patterning along major body axes in other model systems as well.

Although no evidence for connexin genes has been found in invertebrate systems (although see Germain and Ancil, 1996), there are a number of proteins that provide GJC between cells during invertebrate embryogenesis (Phelan and Starich, 2001). Recently, molecular insight has been gained into the basis of GJC in invertebrates. Genes from the family now known as Innexins (formerly called OPUS) comprise a set of important developmental proteins that show no sequence homology to connexins but have the same topology, including four transmembrane domains. The ability of innexins to form functional gap junction channels has been demonstrated directly for a number of innexins (Landesman et al., 1999a; Phelan et al., 1998b; Stebbings et al., 2000). Developmental roles of this gene family have been investigated in *Drosophila* and *Caenorhabditis elegans*, where analysis of genetic mutants implicated innexins in the development of muscle and neuronal cell types (Crompton et al., 1995; Starich et al., 1996; Zhang et al., 1999). These examples of the control of proliferation and patterning by GJC suggest that it as a good candidate mechanism for mediating instructive signals during regeneration.

A primary aspect of regeneration in planaria is the establishment of head/tail identity. The formulation of specific models of long-range signaling in determination of AP polarity requires knowledge of the distribution of signaling pathways that could underlie the exchange of morphogenetic signals. Importantly, a comprehensive expression analysis of all known native genes which could underlie GJC has, to our knowledge,

only been performed in *Drosophila* (Stebbing et al., 2002), but not in any morphogenetic system which offers contexts for highly regulative morphogenesis or regeneration. Moreover, most available data on GJC roles in mammalian and invertebrate models come from deletions of one or at most two GJC gene products, leaving others to mask potentially interesting effects by compensation and/or redundancy. Thus, we cloned the members of the Innexin family in the planarian, *Dugesia japonica*, and comparatively characterized their expression in intact worms and during stages of regeneration. We then performed loss-of-function experiments using reagents that do not distinguish among different innexins to test the role of gap junctions in planarian regeneration, and asked whether GJC is involved in the fundamental determination of anterior–posterior polarity. The induction of bipolar 2-headed animals by exposure to a GJC blocker supports the hypothesis that GJC-based signaling is required for the establishment of correct AP identity during regeneration.

Materials and methods

Worm husbandry

The asexual clonal strain GI of the planarian *D. japonica*, kindly provided by Kiyokazu Agata (Riken, Japan) and Alejandro Sanchez Alvarado (University of Utah, USA), was used in this study. In all experiments, the worms were starved for 1 week before use.

PCR-based cloning of the innexin genes

cDNA from regenerating head and tail fragments of planarians (mixed stages at 1–6 days after cutting) was used as templates for PCR to amplify the planarian innexin genes from a library (5×10^6 independent clones) using the forward primer 5'-CGCGGATCCWSNRRNCARTAYGTNGG-3' and degenerate reverse primer 5'-CGGAATTCGGNACCCAYTGRTARTA-3', corresponding to the highly conserved regions of innexin genes, which the amino acid sequences are (S/T)(K/G)QYVG and YYQWVP, respectively. The PCR amplification was carried out with one cycle at 94°C for 1 min, followed by 40 cycles of 30 s at 94°C, 30 s at 45°C and 30 s at 72°C, and by a final extension at 72°C for 5 min. The library was screened by the PCR-based stepwise dilution method (Watanabe et al., 1997).

Whole-mount *in situ* hybridization

Whole-mount *in situ* hybridization was performed as described previously (Umesono et al., 1999) except for some modifications for greater sensitivity and lower background as follows: prior to prehybridization, the samples were incubated twice in 0.1 M triethanolamine, pH 7.6, for 15 min at RT, and were acetylated using an acetic anhydride series (0.25% and 0.5%) in 0.1 M triethanolamine, pH 7.6, for 15 min each at RT; hybridization was carried out in hybridization solution (50% formamide, $5 \times$ SSC, 100 µg/ml yeast tRNA, 100 µg/ml heparin sodium salt, 0.1% Tween-20, 10 mM DTT, 5% dextran sulfate sodium salt) including about 40 ng/ml digoxigenin (DIG)-labeled antisense riboprobe, that had been denatured at 70°C for 10 min. Chromogenic detection used the BCIP/NBT standard substrates, and was followed by embedding in JB-4 (Polysciences, Inc.) and sectioning at 20 µ.

Drug exposure for GJC inhibition

Intact worms 1–1.5 cm long were put into heptanol (or hexanol) solution (0.0045–0.006% vigorously vortexed into spring water) immediately prior to amputation to equilibrate the worms with the drug solution. The worms were amputated at four levels to generate the head, prepharyngeal, trunk (or

'pharyngeal' according to the scheme of Reddien and Alvarado, 2004), post-pharyngeal and tail fragments. Worm fragments were incubated at 22°C for 2 days. The heptanol solution was exchanged for fresh solution every day. The worms were then washed with water twice and incubated in worm water for 14–20 days to monitor the phenotypes.

Scoring system for anterior–posterior phenotype of regenerates

We developed a quantitative scheme allowing comparison of degree of anteriorization among groups of worms. Each worm was scored on the following scale by observing the posterior blastema: 0 points—normal (a normal worm with a fully-patterned tail), 1 point—weak anteriorization of posterior blastema (missing tail or bipolar pharynx), 2 points—stronger anteriorization of posterior blastema (incomplete ectopic head with eye structures) or 3 points—complete anteriorization of posterior blastema (bipolar head, where the ectopic head has complete development with 2 normal eyes). For each group of worms, we calculated an average score that is the sum of all scores for the worms divided by the total number of worms. For convenience, the index was scaled from 0 to 100 (final index = average score * 100 / 3). On this scale, a group of worms that were all normal would score 0, while a group of worms all of which were fully double-head would score 100. This scheme was focused on ascertaining the extent of anteriorization as judged by external morphology; molecular marker analysis of these phenotypes is presented in Fig. 11.

Results

Isolation and sequences of innexin cDNA

Neither the *Drosophila* and *C. elegans* genome projects (Starich et al., 2001), nor the extensive planarian EST or genome projects (Mineta et al., 2003; Sanchez Alvarado et al., 2002), have located any connexin genes. Therefore, we focused on isolation of innexin genes, which are now known to underlie gap-junctional communication in invertebrates (Dykes et al., 2004; Landesman et al., 1999b; Phelan et al., 1998a,b; Phelan and Starich, 2001). To isolate planarian innexin genes, we first pursued degenerate PCR amplification of innexin gene fragments, using the planarian cDNAs as the templates. We isolated 6 fragments of innexin-like clones, inx1 to 6. We screened a cDNA library to isolate full-length clones. While we isolated and sequenced full-length clones for inx1–5, inx6 was not present in the cDNA library. By searching the planarian *D. japonica* EST database (Mineta et al., 2003), we found an additional 7 putative innexins which were present as incomplete fragments. Based upon these, we screened a cDNA library, and isolated full-length cDNA clones, inx7 to inx13. All cDNA clones included the initiation codon and the 5' and 3' untranslated sequences. The completed sequences of cDNA clones (inx1–5 and inx7–13) and the sequence of PCR fragment of inx6 have been deposited in the DDBJ/EMBL/ GeneBank Library database under accession numbers AB189252–AB189262, AB196957, and AB178521.

Alignment of the predicted amino acid sequences of innexins is shown in Fig. 1. Homology analysis showed that planarian innexins had moderately high homology (50.3–60.5% identity in the conserved region, transmembrane domains 1–4) to *C. elegans* innexin unc-9, except that inx8 and inx11 exhibited 48.1% and 39.8% identity to unc-9, respectively. *D. japonica* inx1 had a high homology (83.1% identity in the 1st–2nd transmembrane domain) to the planarian *Girardia tigrina*

innexin panx1 (Panchin et al., 2000) at the amino acid level, though *D. japonica* inx1 has a stop codon in the middle of the coding region not found in *G. tigrina* panx1, suggesting that *D. japonica* inx1 is the homologue of *G. tigrina* innexin panx1. The conserved four transmembrane domains, cysteine residues in the extracellular loops and tetrapeptide sequence (YYQW, located near the end of the first extracellular loop next to the second transmembrane domain), which exist specifically in all innexin sequences reported so far (Dykes et al., 2004; Phelan and Starich, 2001; Potenza et al., 2002, 2003), were also found in the planarian innexin sequences (Fig. 1), except for *D. japonica* inx1 (because it has a stop codon in the third transmembrane domain). These data indicate that these clones are members of innexin gene family.

Phylogenetic analysis showed the similarity of the planarian innexin sequences to some innexin sequences of Lophotrochozoan (leech, polychaete and mollusc) and *C. elegans* innexins (Fig. 2). Moreover, it showed that the *D. japonica* innexins could be classified into three groups: Group I (inx7 and *G. tigrina* panx1, replacing *D. japonica* inx1), Group II (inx2, inx3, inx4, inx5, inx12 and inx13) and Group III (inx8, inx9, inx10 and inx11). This suggests a homology conservation of innexin genes among animal phyla, and the evolutionary divergence of innexin genes in the planarian. A homology search of the planarian *Schmidtea mediterranea* EST databases (Alvarado et al., 2002, P. Newmark, personal communication) for innexin sequences detected 15 independent clones in the EST databases with significant similarities to innexin genes. Phylogenetic analysis showed that the sequences of 12 of these 15 independent innexin-like clones have significant homology to *D. japonica* inx1–inx4 and inx8–inx13.

Expression characterization of innexin genes

To gain insight into possible roles of GJC in regeneration, we characterized the expression of innexin genes in the planarian using whole-mount in situ hybridization (Figs. 3–9).

Intestine expression of innexins: inx1 and inx7

inx1- and inx7-positive cells were present throughout the anterior and two posterior branches of the intestine (Fig. 3) and changed dynamically during regeneration. In head fragments at 2 days after cutting, inx1 and inx7 were expressed in the two small projections corresponding to the early regenerating posterior branches of the intestine (Fig. 3F). The regenerating branches expressing inx1 and inx7 extended posteriorly (Figs. 3G, H) and the regenerating pharynx appeared in the anterior region between them at 5 days after cutting (Fig. 3H). In 1- to 2-day tail fragments, the intestine branches expressing inx1 and inx7, which had been originally the posterior branches in the intact worms, integrated at an anterior position (Fig. 3I). inx1 and inx7 were also expressed in one small projection that appeared at the anterior position of the integrated branches, corresponding to the early regenerating anterior branch (Fig. 3I). Sectioning clearly showed that the posterior intestine branches at the medial anterior position transitioned to anterior branch by integration of the intestine branches (Figs. 3N, O).

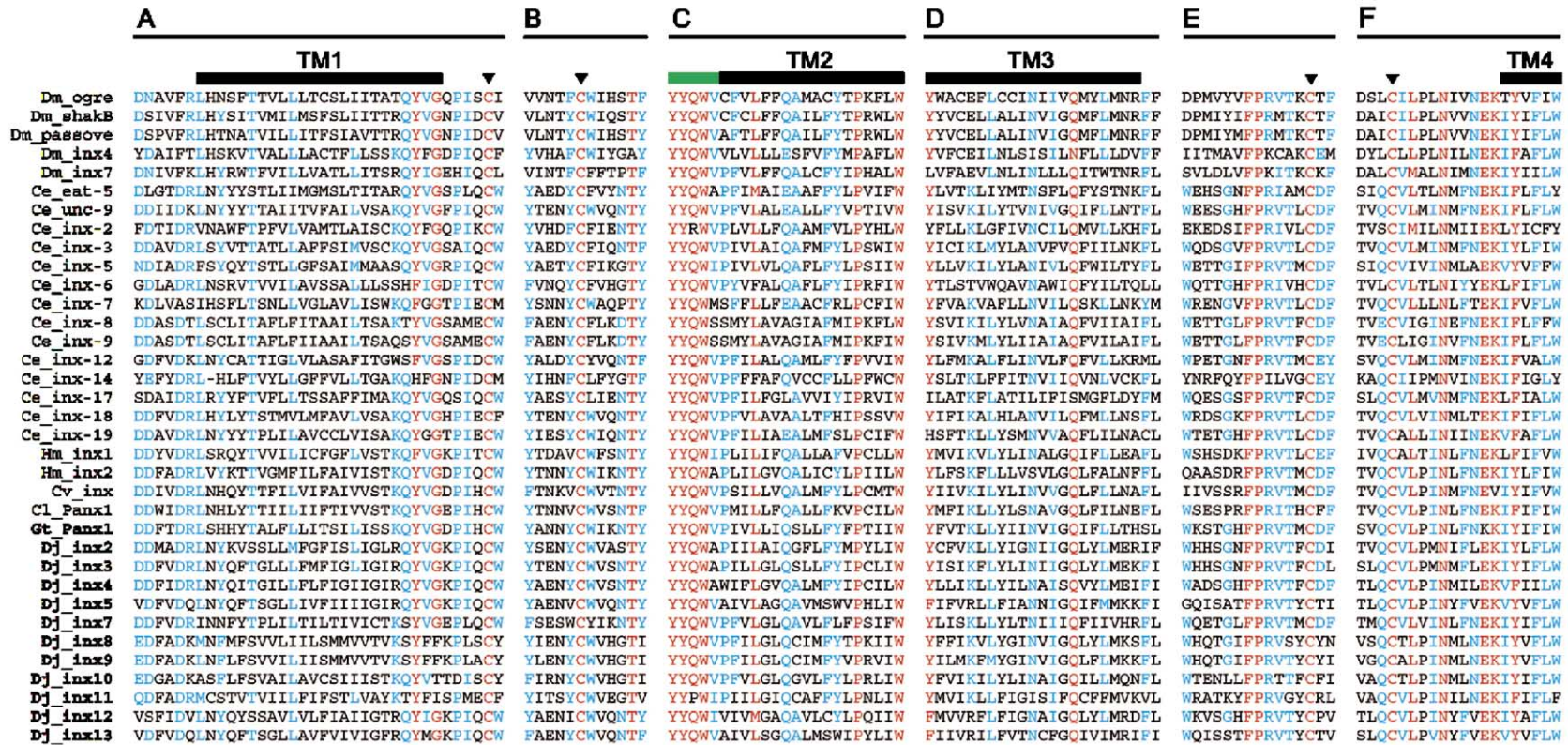


Fig. 1. Alignment of predicted amino acid sequences of innexins. Sequence alignment of innexin proteins showing highly conserved regions. Black bars indicate the predicted transmembrane domains TM1–TM4. Arrowheads indicate conserved cysteine residues in the extracellular loops. High consensus ($\geq 90\%$) amino acids are indicated in red, and the low consensus ($\geq 50\%$) amino acids are indicated in blue. (A) First transmembrane domains and the N-terminal and C-terminal flanking regions. The planarian innexins are highlighted in bold. (B) Conserved regions in the first extracellular loops. (C) Second transmembrane domains and the conserved peptide YYQW(V) at the end of the first extracellular loops. The conserved peptide is indicated by the green bar. (D) Third transmembrane domains and the C-terminal flanking regions. (E) Conserved regions in the second extracellular loops. (F) Part of the fourth transmembrane domains and the conserved region in the second extracellular loops. The multiple alignments were performed utilizing MultAlin v5.4.1 (Corpet, 1988) from the INRA web site (<http://prodes.toulouse.inra.fr/multalin.html>). Dm, *Drosophila melanogaster*; Ce, *Caenorhabditis elegans*; Hm, *Hirudo medicinalis*; Cv, *Chaetopterus varipodatus*; Cl, *Chione limacine*; Gt, *Girardia tigrina*; Dj, *Dugesia japonica*.

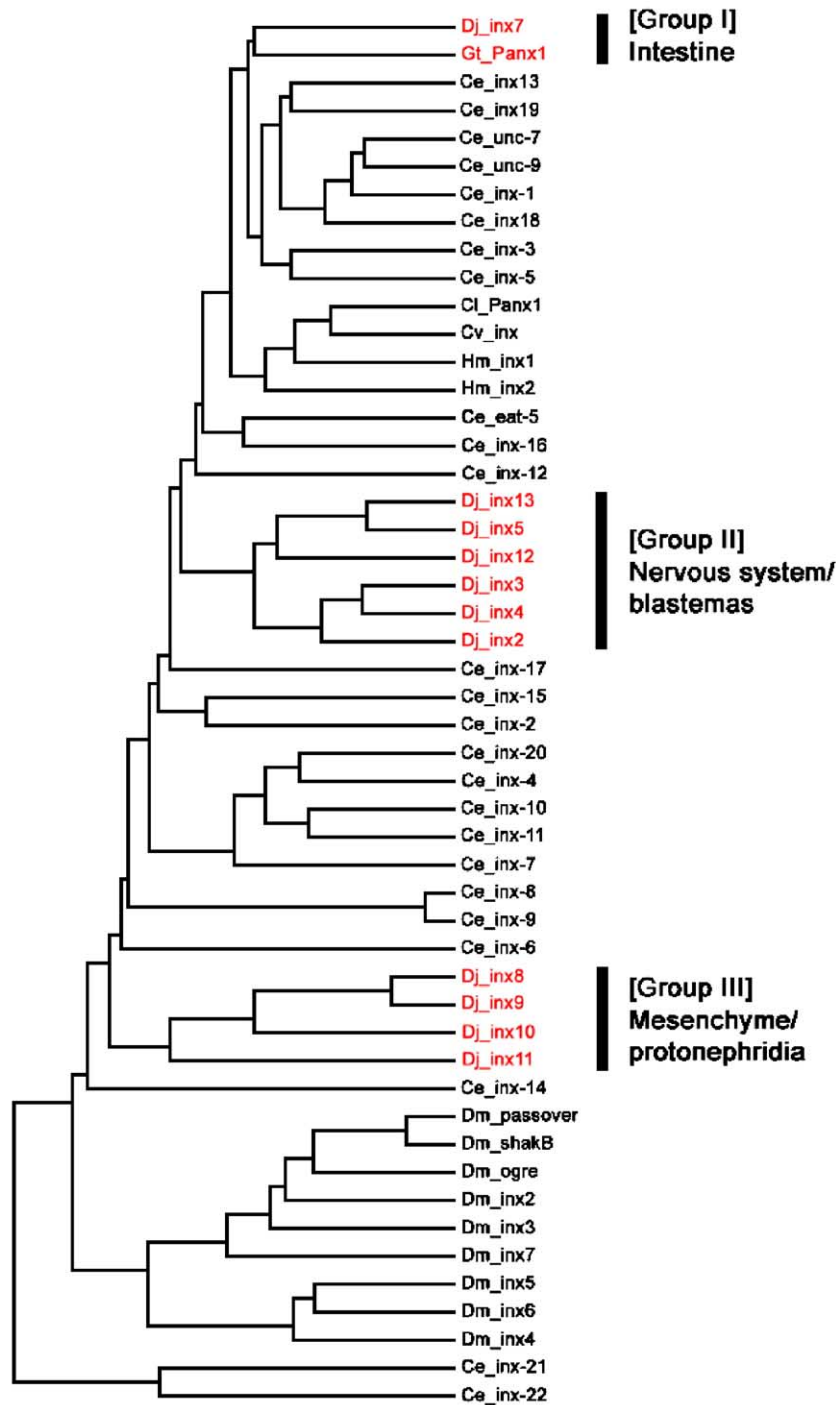


Fig. 2. Phylogenetic tree for innexins. An unrooted tree was constructed using clustering with UPGMA method using GENEYX-MAC software. The predicted amino acid sequences of the conserved region including the whole of the 1st–3rd transmembrane domains (Figs. 1A–E) were used for this analysis. The planarian innexins are highlighted in red. The three groups of the planarian innexin sequences classified by this analysis are indicated by the bars and the names of the groups. Note the remarkable correspondence between clustering the sequences and the gene expression of the planarian innexins (Figs. 3–9). Species names are abbreviated as in Fig. 1.

Nervous system expression of innexins: inx2, inx3, inx4 and inx13

inx2, *inx3*, *inx4* and *inx13* were expressed in the nervous system (Fig. 4), the molecular structure of which has recently been characterized in *D. japonica* (Cebria et al., 2002). Although they were expressed in both the brain and ventral nerve cord (VNC), the distribution of positive cells was

different among these genes. *inx2* was expressed weakly in the medial region of brain and the medial–distal region of brain branches (Figs. 4A, M–O). *inx2* was expressed very weakly in the VNC (Figs. 4A–C). *inx3* was expressed throughout the brain (Figs. 4D, F), and strongly in the medial and lateral regions of the brain and branches (Figs. 4D, P). *inx3* expression extended to the distal region of the brain branches (Figs. 4Q1–

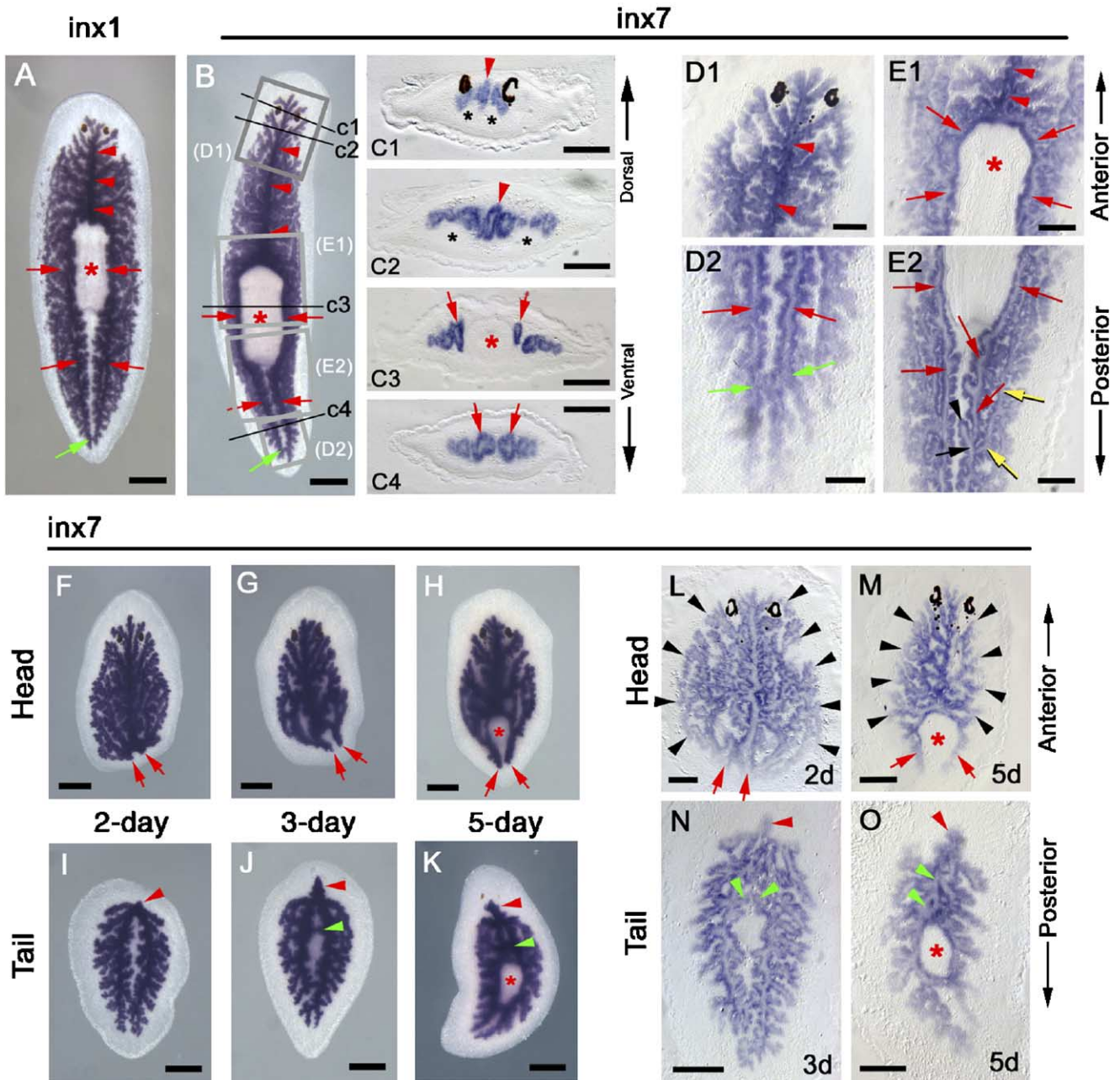


Fig. 3. *inx1* and *inx7* expression in the intestine. Expression of *inx1* (A) and *inx7* (B) in intact worms detected by whole-mount in situ hybridization. Red arrowheads indicate the expression in the intestine branches. Green arrows indicate the bridge connecting two posterior intestine branches at the tail tip. The red asterisk indicates the pharynx. Anterior is to the top. Dorsal view. (C1–C4) Transverse sections; levels are indicated in panel B. The red arrowheads and arrows indicate the expression in the tubular structure of anterior and posterior branches, respectively. The black asterisk indicates the brain. Dorsal to the top. (D1–E2) Horizontal sections. Close-up views of squares D1–E2 in panel B. The red arrowheads and red arrows indicate the expression in the anterior and posterior branches, respectively. In panel E2, one intestine branch (black arrow) diverged to three branches (black arrowhead, red arrow and yellow arrow). Two of the branches (red and yellow arrows) run longitudinally from the branching point. Anterior to the top. (F–K) Expression of *inx7* in the regenerating head fragments and tail fragments at 2 days (F), 3 days and 5 days after cut. Anterior to the top. Dorsal view. (F–H) Head fragments regenerating a tail. The red arrows indicate the regenerating posterior intestine branches. (I–K) Tail fragments regenerating a head. The red arrowheads indicate the regenerating anterior intestine branches. The green arrowheads indicate that the posterior intestine branches are connected by the diverged intestine tracts at the position anterior to the regenerating pharynx. The red asterisk indicates the regenerating pharynx. (L–O) Horizontal sections. Expression of *inx7* in the regenerating head fragments (L, M) and tail fragments (N, O) at 2 days (L), 3 days (N) and 5 days (M, O) after cutting. The red arrows indicate the regenerating posterior intestine branches. Red arrowheads indicate the regenerating anterior intestine branches. The black arrowheads indicate the diverging pattern of intestine branches in the head fragments. Note that the diverging pattern is simplified in the region anterior to the regenerating pharynx at 5 days after cutting in panel M, compared to 2 day after cutting in panel L. The green arrowheads indicate that the posterior intestine branches are integrated at the middle–center position anterior to the regenerating pharynx. Anterior is to the top. Scale bars: A, B—300 μ m; C1–C4—200 μ m; D1—200 μ m; D2—100 μ m; E1, E2—250 μ m; F–K—300 μ m; L–O—200 μ m.

R). *inx3* was expressed in the VNC, though the intensity of expression was very low in intact worms (Fig. 4D), compared to the high expression observed during regeneration (Figs. 4E–F).

inx4 was expressed in the brain branches and the medial and lateral regions of the brain (Figs. 4G, S). In contrast to *inx2* and *inx3*, *inx4* was expressed in neuron-like cells throughout the peripheral region of the head, where sensory organs are aligned and project to the brain branches (Figs. 4T1–U). *inx4* was expressed in the posterior blastema at 5 days after cutting (Fig. 4I). *inx4* was also expressed in the VNC (Figs. 4G–I), being up-regulated in the anterior region at 5 days after cutting (Fig. 4I). *inx4* was expressed in a number of cells throughout the body; especially strong expression was detected in the photoreceptor cells that plug the eyecup of the pigment cells (Figs. 5A–C), contrasting with the absence of expression of the other innexins in the photoreceptor cells (Fig. 5D). During regeneration, the expression of *inx4* in the photoreceptor cells began at 4 days after cutting (Fig. 5E) prior to the appearance of maturely pigmented eyecup at 5 days after cutting.

inx13 was expressed in the lateral and medial region of the brain (Figs. 4J, L). In intact worms, the expression in the lateral region was much higher than in the medial region (Figs. 4V, W1). It was expressed in the brain branches, though the expression was restricted to the stem region (Figs. 4W1, X). Expression of *inx13* in the VNC was very weak, but was up-regulated in the posterior region in the VNC during regeneration (Figs. 4K, L). Alongside the expression in the nervous system, these genes were expressed in the pharynx, in which a number of neuronal cells exist: *inx2* (Figs. 4A–C), *inx3* (Figs. 4D–F) and *inx13* (Figs. 4J–L) were expressed in the posterior region in the pharynx, while *inx4* was expressed in the anterior and posterior regions (Figs. 4G–I). This contrasts with expression of the intestine-type innexins (*inx1*, *inx7*) that were not expressed in the pharynx, even though the pharynx connects directly to the intestine ducts (Fig. 3).

Innexin expression in the regenerating brain: inx2, inx3, inx4 and inx13

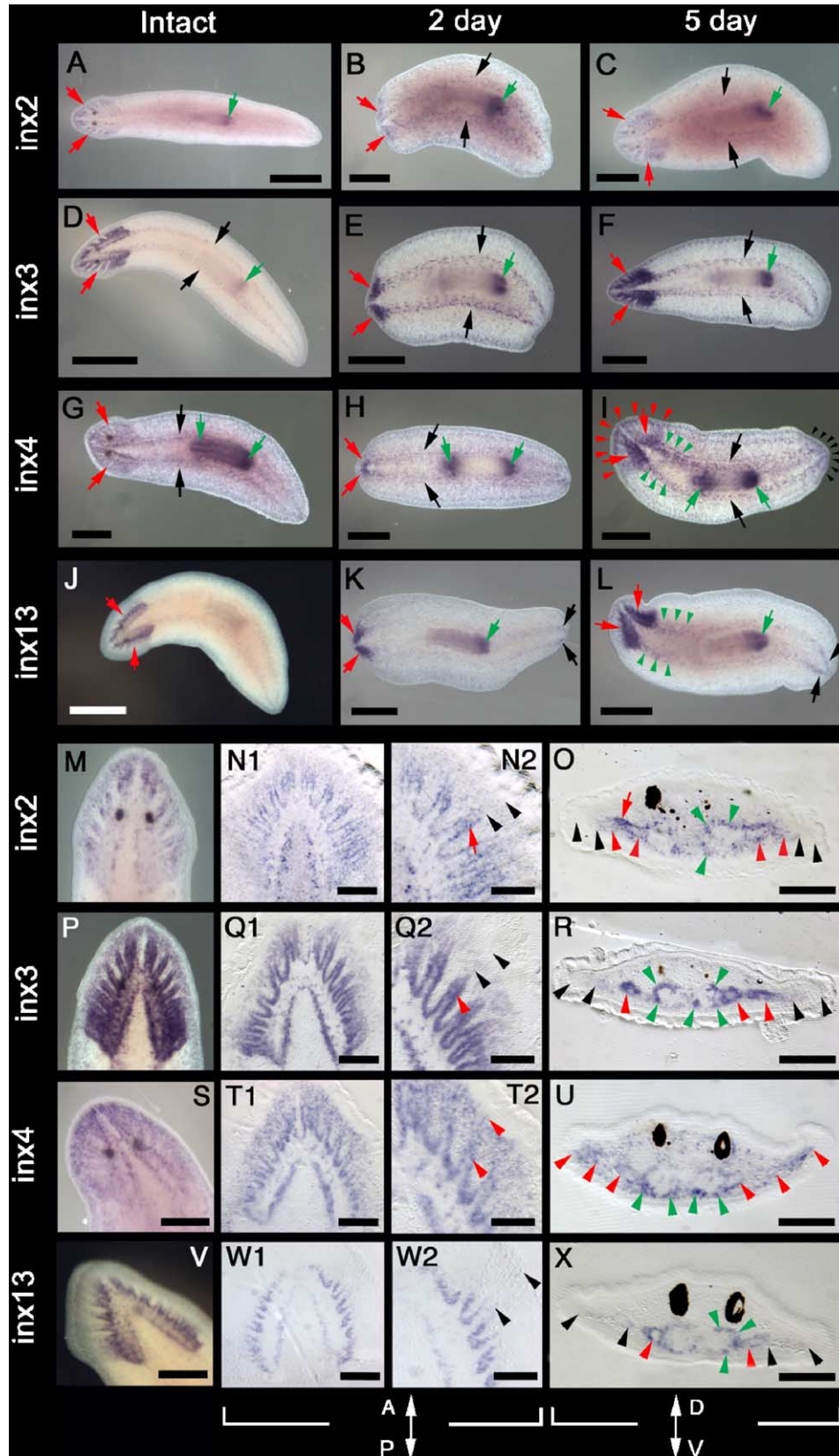
The expression of *inx2*, *inx3*, *inx4* and *inx13* changed dynamically during brain regeneration (Fig. 6), allowing classification into two categories: early (initiating in the regenerating brain within 1 day after cutting) and late (initiating at 2 days after cutting). *inx2* and *inx4* were late genes. The expression of *inx2* was initiated in the medial and lateral region of the regenerating brain at 2 days after cutting (Fig. 6A2). At 3 days to 4 days after cutting, *inx2* was expressed in the broad region regenerating the brain branches in the anterior blastema, though the branching pattern was not clear yet (Figs. 6A3, A4). The expression of *inx4* was initiated at the anterior–medial region of the regenerating brain at 2 days after cutting (Fig. 6B2). This contrasts with the expression of the brain marker *DjotxB*, which is expressed in the middle- and posterior-lateral region of the regenerating brain at the same stage of regeneration (Umesono et al., 1999). At 3 to 5 days after cutting, *inx4* was expressed in the medial region of the regenerating brain, extending the expression posteriorly in the medial region of the regenerating brain (Figs. 6B3, B4, B5). Interestingly, the expression of *inx4* was up-regulated transiently in the medial region of the regenerating brain at 4 days after cutting (Fig. 6B4).

In contrast, *inx3* and *inx13* were early genes, and expression was first detected at 18 h and 1 day after cutting, respectively. The expression of *inx3* initiated in the early regenerating brain in the anterior region of the blastema within 1 day (Fig. 6C1). The earliest detectable signal was seen at 18 h after cutting. At 2 days, *inx3* was expressed in the medial and lateral region of the regenerating brain. The expression was extended posteriorly in both of the medial and lateral region of the regenerating brain (Fig. 6C2). At 4 to 5 days, the strong expression of *inx3* delineated clearly the structure of brain branches (Figs. 6C4, C5). The expression of *inx13* initiated in the early regenerating

Fig. 4. *inx2*, *inx3*, *inx4* and *inx13* expression in the nervous system. Panels A–L show whole-mount views of intact worms and regenerating trunk worm fragments (at 2 days and 5 days after cut, indicated by 2d and 5d, respectively). Red arrows indicate the expression in the brain of intact worms and regenerating worms at 2 days after cutting. Anterior to the left. Ventral view. (A–C) Expression of *inx2*. (D–F) Expression of *inx3*. In panels D and E, the black arrows indicate the expression in the VNC in the intact worm (D) and regenerating worm at 2-day after cut (E). Note that the expression in the VNC is up-regulated during regeneration. (G–I) Expression of *inx4*. In panel G, the black arrows indicate the expression in the VNC in the intact worm. In panel I, the black arrows indicate that the expression is up-regulated in the anterior region of the VNC, and the black arrowheads indicate the expression in the posterior blastema at 5 days after cutting. (J–L) Expression of *inx13*. In panels K and L, the black arrows indicate the expression in the regenerating VNC in the posterior blastema. (M–O) Expression of *inx2* in the head region in the intact worm. (M) Close-up view of the head. Anterior to the top. Ventral view. (N1, N2) Horizontal section. Close-up view of the brain and brain branch, respectively. In panel N2, the red arrows indicate expression in the medial–distal region of the brain branch. The black arrowheads indicate expression that does not extend to the peripheral region. Anterior to the top. (O) Transverse section at the level of the eyes. The green arrowheads indicate the expression in the brain. The red arrow indicates the strong expression at the medial–distal region of brain branch. Dorsal to the top. (P–R) Expression of *inx3* in the head region in the intact worm. (P) Close-up view of the head. Anterior to the top. Ventral view. (Q1, Q2) Horizontal section. Close-up view of the brain and brain branch, respectively. In panel Q2, red arrows indicate expression in the distal region of the brain branch. The black arrowheads indicate that the expression does not extend to the peripheral region. Anterior to the top. (R) Transverse section at the level of the eye. The green arrowheads indicate the expression in the brain. The red arrowheads indicate the expression in the brain branches. The black arrowheads indicate that the expression does not extend to the peripheral region. Dorsal is to the top. (S–U) Expression of *inx4* in the head region in the intact worm. (S) Close-up view of the head. Anterior is to the top. Ventral view. (T1, T2) Horizontal section. Close-up view of the brain and brain branch, respectively. In panel T2, the red arrowheads indicate expression in the brain branch and peripheral neurons. Anterior is to the top. (U) Transverse section at the level of the eye. The red arrowheads indicate the expression in the brain branches and peripheral neurons. The green arrowheads indicate the expression in the medial and lateral region at the ventral side in the brain. (V–X) Expression of *inx13* in the head region in the intact worm. (V) Close-up view of the head. Anterior is to the top. Ventral view. (W1, W2) Horizontal section. Close-up view of the brain and brain branch, respectively. In panel S, the black arrowheads indicate that expression is absent in the region between the black arrowheads in the brain branch. Anterior is to the top. (X) Transverse section at the level of the eye. The green arrowheads indicate the expression in the lateral region in the brain. The red arrowheads indicate the expression in the proximal region of the brain branches. The black arrowheads indicate the absence of the expression in the region between the black arrowheads in the brain branch. Scale bars: A, D, J—750 μ m; B, C, E–I, K, L—500 μ m; M, P, S, V—200 μ m; N1, Q1, T1, W1, O, R, U, X—100 μ m; N2, Q2, T2, W2—50 μ m.

brain in the anterior region of the blastema at 1 day after cutting (Fig. 6D1). At 2 days after cutting, *inx13* was expressed in the medial and lateral region of the regenerating brain (Fig. 6D2). At 3 days, *inx3* was expressed in the stems of early

regenerating brain branches (Fig. 6D3). At 4 to 5 days after cutting, the expression of *inx13* in the regenerating brain branches grew out peripherally, following the regeneration of the brain branches, but did not extend completely to the tip of



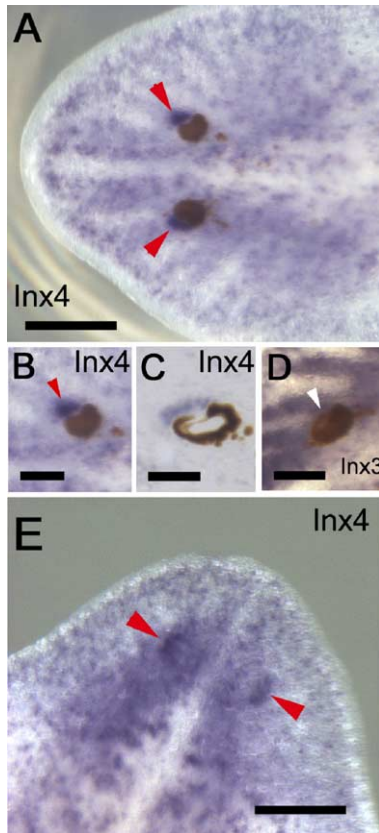


Fig. 5. *inx4* expression in photoreceptor cells. (A–C) Expression of *inx4* in the intact worm. The red arrowheads indicate the expression in the photoreceptor cell plugging the pigmented eyecup. Anterior is to the left. Dorsal view. (A) Close-up view of the head the whole-mount specimen. (B) Close-up view of the eye. (C) Horizontal section. Close-up view of the eye. (D) Expression of *inx3* in the intact worm. Close-up view of the eye. The white arrowhead indicates the absence of the *inx3* expression. Note that *inx3* is expressed strongly in brain cells just under the eye. Anterior is to the left. Dorsal view. (E) Expression of *inx4* during regeneration. 4 days after cutting. The red arrowheads indicate the expression in the cells in the regenerating photoreceptor. Note that the pigmented eye cups have not appeared clearly yet. Anterior to the top. Dorsal views. Scale bars: A, E—200 μ m; B, D—75 μ m; C—50 μ m.

the brain branches (Figs. 6D4, D5; compare to Figs. 6C4, C5). This was similar to the expression of CNS marker DjPC2 (Agata et al., 1998) in the regenerating brain branches at the same stages (Figs. 6E4, E5).

Expression of innexins in the blastema: *inx5* and *inx12*

In intact worms, *inx5* was expressed at the edge of the head where sensory organs are aligning (Figs. 7A, D, J and 4S) and in the scattered cells distributing throughout the dorsal side of the body (Figs. 7A, N), exhibiting graded distribution from the head to tail along the AP axis (Figs. 7J, K), and in a number of cells along the VNC, with a dense distribution along the VNC in the head region (Figs. 7D, N). During regeneration, *inx5* was expressed in the blastema. At 2 days after cutting, *inx5* was initially expressed at the edge of the anterior blastema and in some scattered blastema cells (Figs. 7B, E, L). Sectioning revealed that *inx5* was expressed at the leading edge of head mesenchyme in the regenerating head (Fig. 7O). Following brain regeneration, the *inx5*-positive cells appeared at a high

density along the VNC in the regenerating head region (Fig. 7F) and in the regenerating tail region (Fig. 7F).

In contrast, *inx12* was expressed very weakly in the head and tail region in intact worms (Fig. 7G). During regeneration, *inx12* was expressed in both of the anterior and posterior blastema and weakly in the midline in the posterior region of the body (Figs. 7H, I). Sectioning revealed that *inx12* was expressed in the mesenchyme anterior to the regenerating intestine in the anterior blastema at 2 days after cutting (Fig. 7M). At 5 days after cutting, the expression level of *inx12* was reduced in the blastema, and the expression was mostly restricted at the edge of the regenerating head (Fig. 7I). Following brain regeneration, *inx12* was expressed in cells outlining the VNC in the regenerating head (Fig. 7I).

inx8, *inx9* and *inx11* expression in the mesenchyme

inx8 and *inx9* were expressed in the mesenchyme throughout most of the body but not in the intestine (Figs. 8A, D). *inx8* and *inx9* were expressed in the mesenchyme between the epithelium/muscle, intestine and nervous system (Figs. 8A, J–L, D, M–O), though there were some differences: *inx8* was strongly expressed in some mesenchyme cells around and between the small branches of intestine (Figs. 8J–L) and between the intestine branch and pharynx (Fig. 8K), as well as in the pharynx; *inx9* was more ubiquitously expressed in the mesenchyme (Figs. 8M–O), but not expressed between the intestine branch and pharynx (Fig. 8N). Both *inx8* and *inx9* were strongly expressed in the mesenchyme tissue around the pharynx and at the midline in the tail region (Figs. 8A, D). Although *inx8* and *inx9* were strongly expressed in the regenerating head and tail at a late stage of regeneration (Figs. 8C, F), *inx9* was highly expressed in the anterior blastema (Figs. 8E, P). Sectioning revealed *inx9* in the thin mesenchyme layer outlining the anterior part of the regenerating intestine in the anterior blastema at 2 days after cutting (Fig. 8Q). *inx11* was also expressed in the mesenchyme (Figs. 8G–I). Expression was absent from the nervous system and intestine (Figs. 8R–U). Also, *inx11* expression was absent from the mesenchyme (except the edge and midline) in the tail tip of the intact worms (Fig. 8G) and in the posterior blastema during regeneration (Figs. 8H, I). Additionally, *inx11* was strongly expressed in the dorsal midline of the body (Fig. 8G). Distinct from *inx8* and *inx9*, the expression of *inx11* was restricted to the medial region in the head mesenchyme (Figs. 8G, R).

inx10 expression in the protonephridia

inx10 was expressed in a number of small thread-like structures mainly in the lateral–peripheral region in the intact worms (Figs. 9A–C). The threadlike structures were sparsely distributed in the mesenchyme tissue underneath the epithelium (Fig. 9D). This was similar to the known distribution of the protonephridia observed in electron microscopy studies reported previously (Hyman, 1951; Ishii, 1980). During regeneration, the shape of threadlike structures expressing *inx10* changed dynamically in the blastemas (Figs. 9E–K). *inx10* was expressed also in the anterior and posterior regions of the pharynx (Fig. 9A), similarly to the expression as *inx4* (Figs. 4G–I).

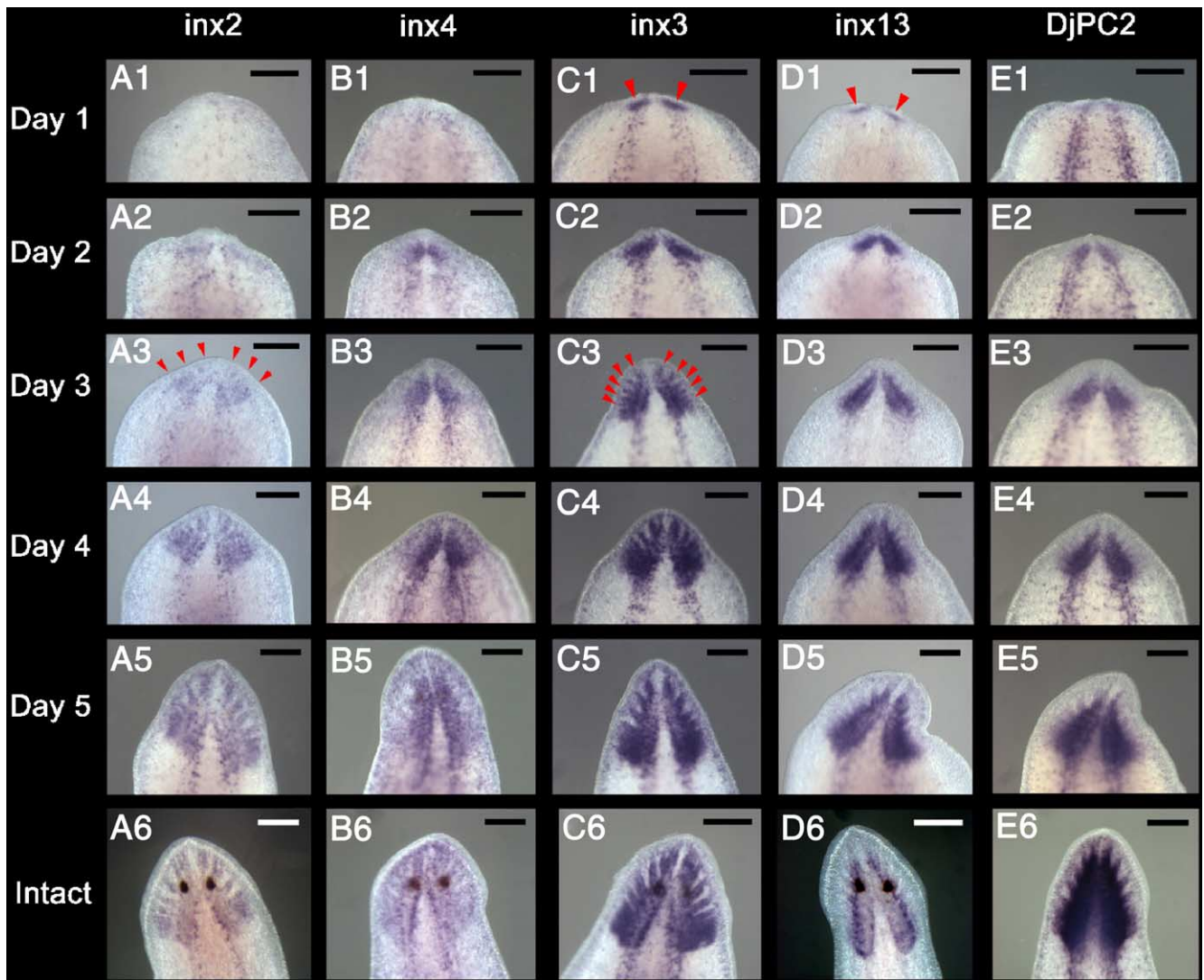


Fig. 6. *inx2*, *inx3*, *inx4* and *inx13* expression in the brain during regeneration. *inx2*, *inx3*, *inx4* and *inx13* expression in cephalic regenerates (1 day to 5 days after cut). Close-up view of the anterior region of the regenerating trunk fragments and intact worms. Anterior is to the top. Ventral view. (A1–A6) Expression of *inx2*. (B1–B6) Expression of *inx4*. (C1–C6) Expression of *inx3*. (D1–D6) Expression of *inx13*. (E1–E6) Expression of the CNS marker DjPC2. In panels C1 and D1, red arrowheads indicate that the expression of *inx3* and *inx13* is initiated in the early regenerating brain, respectively. In panels A3 and C3, the red arrows indicate the expression of *inx2* and *inx3* in the regenerating brain branches, respectively. Scale bars are 200 μm .

Functional analysis of GJC on planarian regeneration by inhibitor treatment

To test the hypothesis that GJC was required for correct patterning during regeneration, we sought a loss-of-function reagent that would affect all gap junctions. Currently-popular RNAi approaches are not well-suited for this purpose because they target individual innexin transcripts and it is not currently possible to combine RNAi targeting all 13 transcripts in one animal. Indeed, recent large-scale RNAi screens in planaria did not uncover roles of innexin genes (Reddien et al., 2005). Our expression data indicated overlapping expression domains of members of this large family; thus, inhibition by RNAi may mask interesting functional roles of gap junctions because of functional redundancy and possible compensation effects among the different innexins. Thus, we chose heptanol, a classical reagent for disrupting GJC that also has the advantage of ease of application, allowing large numbers of worms to be

tested (necessary for the experiments below). Heptanol and other long-chain *n*-alkanols are efficient and rapidly-reversible blockers of both electrical and chemical GJC in both connexin- (Chanson et al., 1989; Levin and Mercola, 1998) and innexin-based gap junctions (Adler and Woodruff, 2000; Anderson and Woodruff, 2001; Brooks and Woodruff, 2004; Bukauskas et al., 1992; Carrow and Levitan, 1989; Mire et al., 2000; Peracchia, 1991; Weingart and Bukauskas, 1998; Yazaki et al., 1999).

We treated regenerating worms at an early stage of regeneration (2 days after cutting) with 1–10 μM heptanol dissolved in the medium. In all experiments, the heptanol concentration was sufficiently low to cause no general ill effects on worm health as observed by macroscopic observation. No effects were observed on intact worms. At 7 days post-cutting, we assayed the worms for the morphology of blastemas. Trunk fragments of worms exposed to heptanol exhibited clear anteriorization of both blastemas in 43% of the

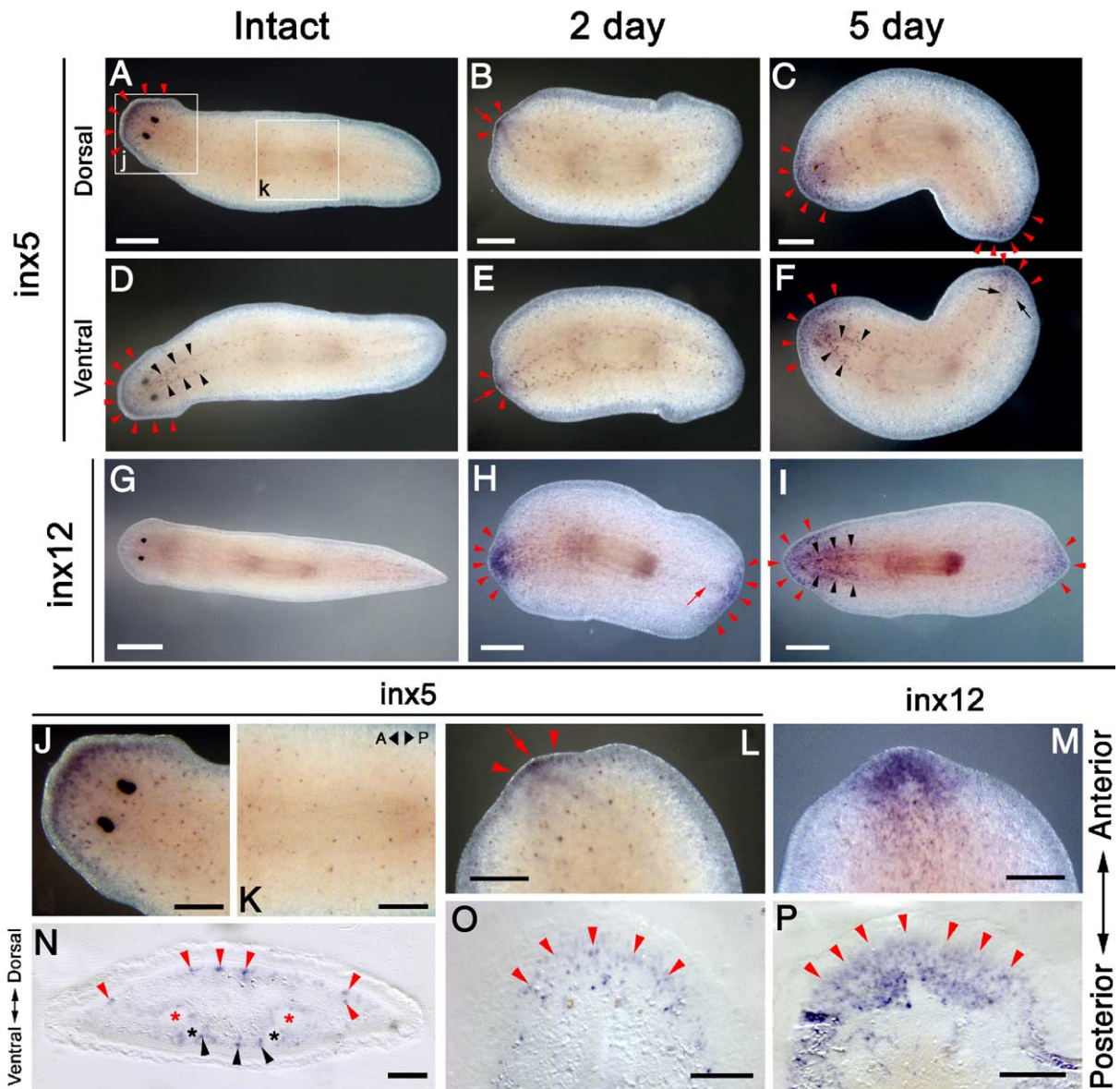


Fig. 7. Expression of *inx5* and *inx12* in the blastema. Expression of *inx5* and *inx12* in the blastema. Panels A–I are whole-mount views of the intact worms and regenerating trunk worm fragments (at 2 days and 5 days after cutting). Anterior is to the left. (A–C) Expression of *inx5*. Dorsal view. (A) Intact worm. The red arrowheads indicate the expression in the anterior edge of the head. (B) 2 days after cutting. The red arrowheads indicate the expression in the edge of the anterior blastema. The strongest expression at the tip of the blastema is indicated by the red arrow. (C) 5 days after cutting. The red arrowheads indicate the expression in the edges in the anterior and posterior blastemas. (D–F) Expression of *inx5*. Ventral view. (D) Intact worm. *inx5* is expressed in some cells along the VNC, especially in the head region indicated by the black arrowheads. (E) 2 days after cutting. (F) 5 days after cutting. The black arrowheads indicate the expression in some cells along the VNC in the regenerating head and tail. (G–I) Expression of *inx12*. (G) Intact worm. Dorsal view. (H) 2 days after cutting. The red arrowheads indicate the expression in the anterior and posterior blastemas. The red arrow indicates the weak expression in the midline in the posterior region of the worm fragment. Dorsal view. (I) 5 days after cutting. The red arrowheads indicate the expression in the regenerating head and tail. Ventral view. The black arrowheads indicate the expression in the cells outlining the VNC in the regenerating head. Ventral view. (J–O) Expression of *inx5*. (J, K) Close-up view of head region and trunk region of the intact worm indicated by the square j and k in panel A. The anterior–posterior direction was indicated as A and P. Note that the density of *inx5*-positive cells is different between panels J and K. Dorsal view. (N) Transverse section at the head region of the intact worm. The red arrowheads indicate the scattered cell expressing *inx5* at the dorsal side of the body. The black arrowheads indicate the expression of *inx5* in the cells along the VNC in the head region. The red asterisks indicate the brain. The black asterisks indicate the VNC. Dorsal to the top. (L, O) Expression of *inx5*. Magnified view of the anterior blastemas of the regenerating trunk fragments. Anterior to the top. (L) Whole-mount specimen at 2 days after cutting. The red arrowheads and red arrow indicate as panel B. Dorsal view. (O) Horizontal section of the regenerating trunk fragment at 5 days after cutting. The red arrowheads indicate the expression at the leading edge of the anterior mesenchyme. Note that some *inx5*-positive cells are scattered in the mesenchyme posterior to the edge. (M, P) Expression of *inx12*. Close-up view of the anterior blastema of the regenerating trunk fragments at 2 days after cutting. Anterior is to the top. (M) Whole-mount. Dorsal view. (P) Horizontal section. The red arrowheads indicate the expression in the mesenchyme anterior to the regenerating intestine. Scale bars: A, D—400 μ m; B, C, E, F—300 μ m; G—500 μ m; H, I—300 μ m; J–M, O, P—200 μ m; N—100 μ m.

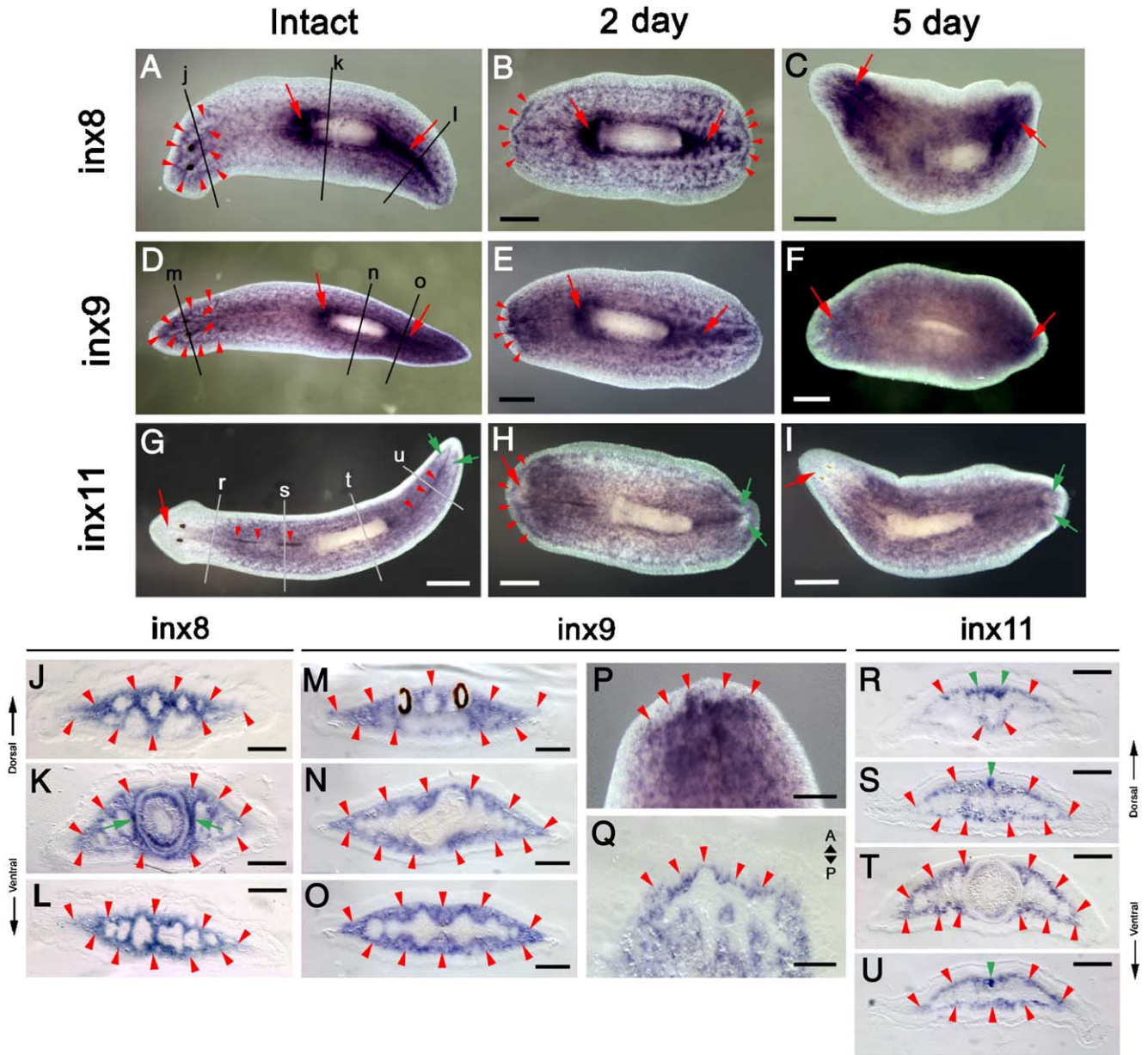


Fig. 8. *inx8*, *inx9* and *inx11* expression in the mesenchyme. *inx8*, *inx9* and *inx11* expression in the mesenchyme. Panels A–I show whole-mount specimens. (A–C) Expression of *inx8*. Dorsal view. (A) Intact worm. The red arrows indicate the strong expression in the mesenchyme around the pharynx and in the midline posteriorly to the pharynx. The red arrowheads indicate that the expression is clearly in the mesenchyme between the small intestine branches in the head region (compare to Figs. 3A, B). (B) 2 days after cutting. The red arrows indicate the strong expression in the mesenchyme around the pharynx. The red arrowheads indicate expression in the narrow region of the mesenchyme in both blastemas. (C) 5 days after cutting. Red arrows indicate strong expression in the mesenchyme in the regenerating head and tail. (D–F) Expression of *inx9*. Dorsal view. (D) Intact worm. The red arrows and red arrowheads indicate the expression of *inx9* in the mesenchyme that is similar to *inx8*. (E) 2 days after cutting. The red arrowheads indicate the strong expression in the mesenchyme in the anterior blastema. (F) 5 days after cutting. The red arrows indicate the strong expression in the mesenchyme in the regenerating head and tail. (G–I) Expression of *inx11*. Dorsal view. (G) Intact worm. The red arrow indicates that expression is absent from the head region. Green arrows indicate that *inx11* is expressed in a few cells in the mesenchyme, excluding the edge and midline, in the tail tip. Red arrowheads indicate the expression in the dorsal midline. (H) 2 days after cutting. The red arrow indicates that the expression is absent from the anterior blastema, excluding the edge indicated by the red arrowheads. Green arrows indicate the expression absent from a pair of small domains in the posterior blastema. (I) 5 days after cutting. Red arrow indicates that the expression is absent from the regenerating head region. The green arrows indicate that *inx11* is expressed in a few cells in the tip of the regenerating tail region. (J–L) Expression of *inx8*. Transverse sections of intact worm at the levels of the head (J), trunk (K) and tail (L), which are indicated in panel A. The red arrowheads indicate the expression in the mesenchyme. The green arrows indicate the strong expression in the mesenchyme between the intestine branches and pharynx. Dorsal upwards. (M–Q) Expression of *inx9*. (M–O) Transverse plastic section of intact worm at the levels of the head (M), trunk (N) and tail (O), which are indicated in panel D. Red arrowheads indicate the expression in the mesenchyme. Dorsal upwards. (P) Close-up view of the anterior blastema of the trunk fragment at 2 days after cutting. Red arrowheads indicate the strong expression in the mesenchyme in the anterior blastema. Anterior to the top. (Q) Horizontal section of the trunk fragment at 2 days after cutting. Close-up view of the anterior blastema. Red arrowheads indicate expression in the thin mesenchyme layer outlining the anterior part of the regenerating intestine in the anterior blastema. Anterior is to the top. (R–U) Expression of *inx11*. Transverse plastic section of intact worm at the level of the posterior part of the head (R), anterior to pharynx (S), pharynx (T) and tail (U), which are indicated in panel G. Red arrowheads indicate expression in the thin mesenchyme layer. In panel R, the green arrowheads indicate the expression in the dorso-medial region of the mesenchyme. In panels S and U, the green arrowheads indicate the strong expression in the mesenchyme layer in the dorsal midline. Dorsal side is upwards. Scale bars: A–C—300 μ m; D—500 μ m; E–I—300 μ m; J–L—200 μ m, M–P—100 μ m; Q—50 μ m; R–U—200 μ m.

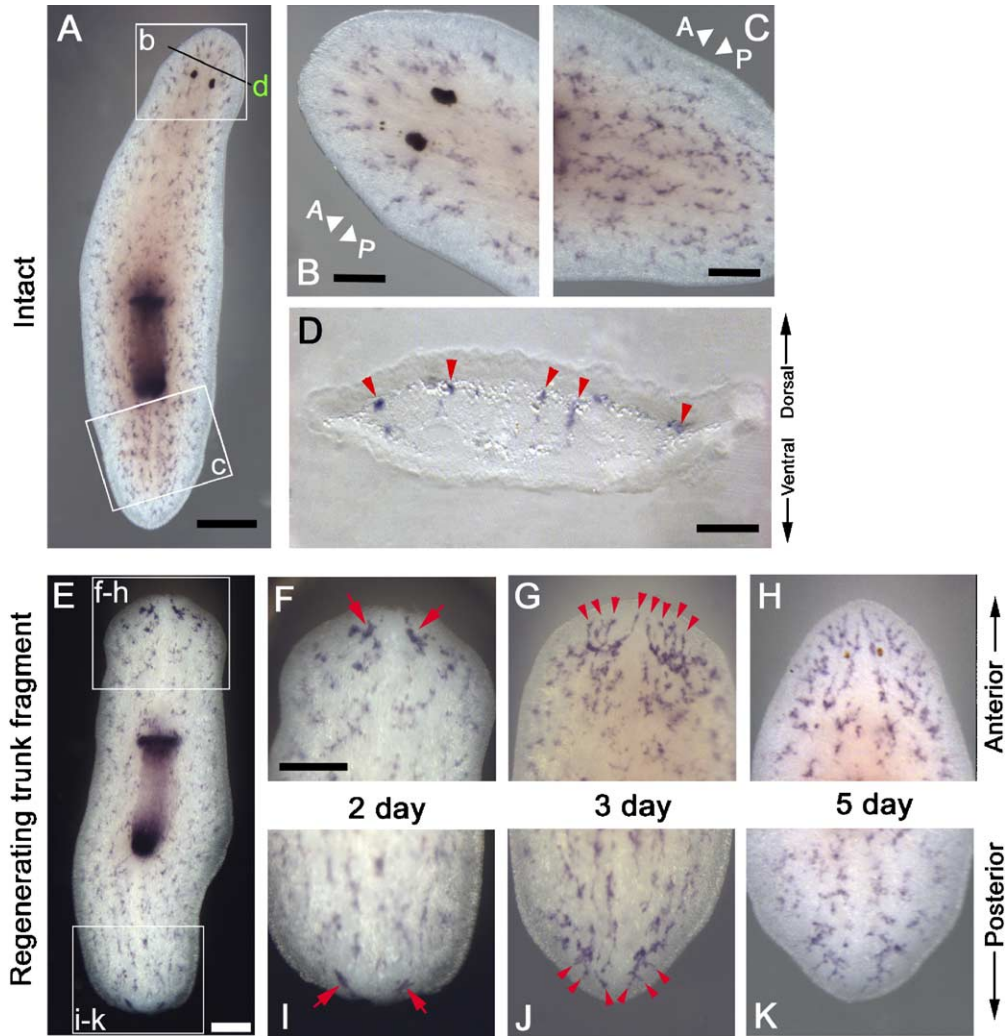
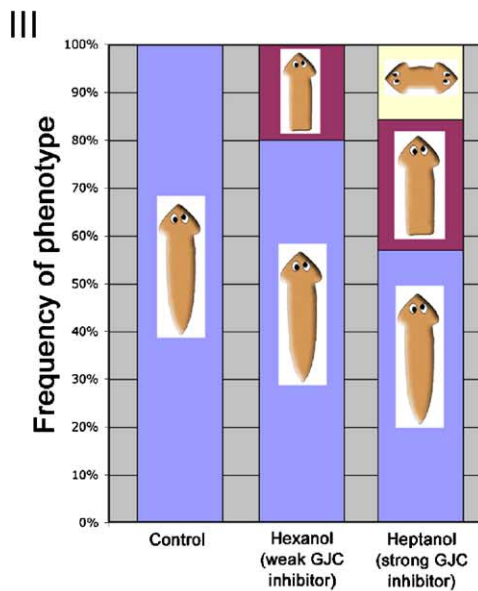
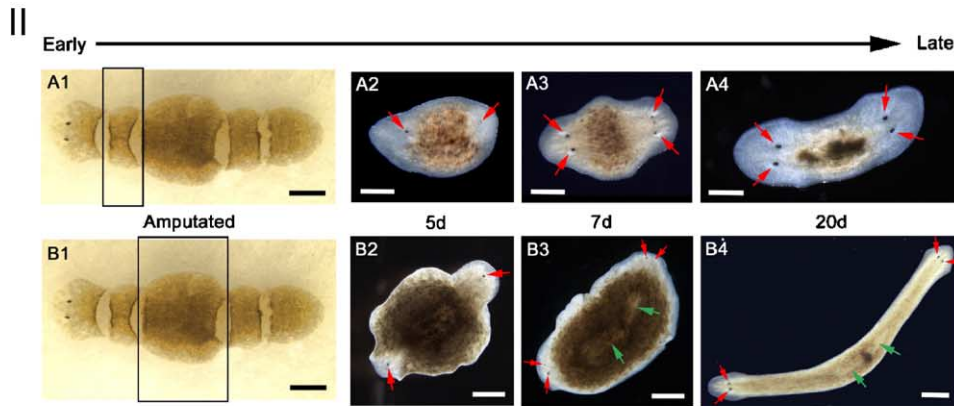
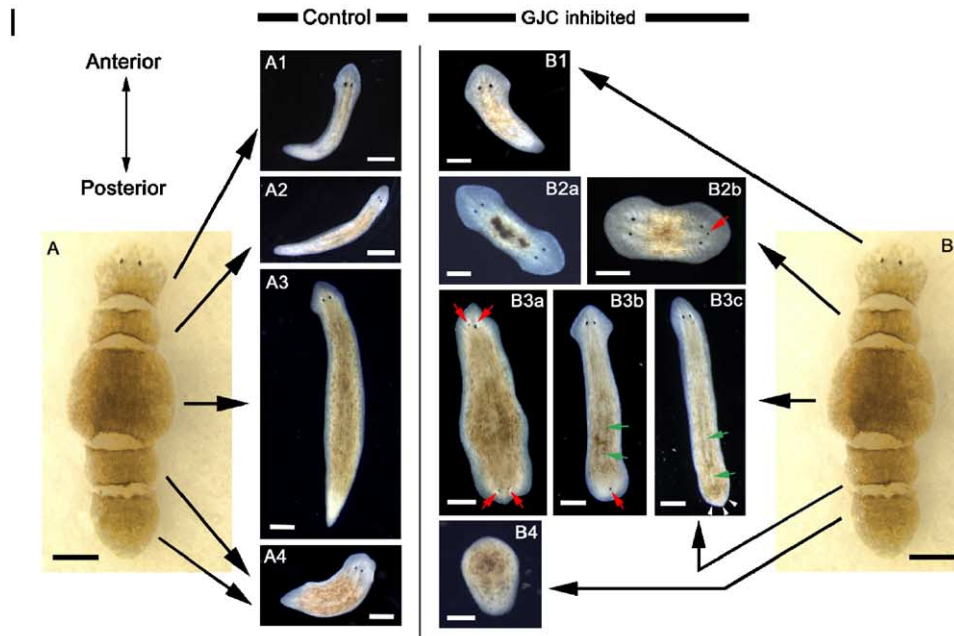


Fig. 9. *inx10* expression in the protonephridia. Panels A–D show intact worms. (A) Whole-mount; anterior to the top; dorsal view. (B) Close-up view of the head (square b in panel A). Anterior to the left. Dorsal view. (C) Close-up view of the tail (square c in panel A). Anterior to the left. Dorsal view. The *inx10*-positive cells are not in the midline. (D) Transverse section of the specimen at the level of the head. Dorsal is to the top. The red arrows indicate the *inx10*-positive cells in the mesenchyme underneath the epithelium. (E–K) Regenerating trunk fragments. (E) Whole-mount view of the regenerating trunk fragment at 2 days after cutting. Dorsal view. (F–K) Expression changes in the anterior blastemas (as shown in squares f–h in panel E) and posterior blastemas (as shown in squares i–k in panel E) were monitored and shown in panels F–H and I–K, respectively. In panels F–H, anterior is to the top. In panels I–K, posterior is to the bottom. (F, I) 2 days after cutting. Red arrows indicate that *inx10* is expressed in a pair of the rod-like structures in the blastemas. (G, J) 3 days after cutting. The red arrowheads indicate that *inx10* is expressed in the small branches extending from the rod-like structure in the blastemas (H, K) 5 days after cutting. Scale bars: A—300 μ m; B–D—100 μ m; E–K—150 μ m.

Fig. 10. Morphogenetic effects of GJC inhibition on regeneration. Phenotypes observed in worms treated with GJC blockers. (I) Position dependence of the phenotypes. Intact worms were amputated at four levels to make five body fragments: head, prepharyngeal, trunk (including the pharynx), post-pharyngeal and tail fragments, in the order of top to bottom in panels I-A and I-B. Dorsal view. (I-A1–I-A4) Control worms that were regenerated from the each worm fragment shown in panel I-A. 20 days after cutting. (I-B1–I-B4) Phenotypes that were generated from each GJC-inhibited worm fragment are shown in panel I-B. 20 days after cutting. Dorsal view. (I-B1) Normal morphology of the worm from the head fragment. (I-B2a, I-B2b) Bipolar head phenotypes of prepharyngeal fragments. The red arrow indicates the ectopic eye in I-B2b. (I-B3a–I-B3c) Bipolar phenotypes of the trunk fragments and post-pharyngeal fragments. The green arrows indicate the bipolar pharynxes. The pharynxes are not obvious in the worm in I-B3a. (I-B3a) Severe bipolar head phenotype of the trunk fragments. The red arrows indicate that there are pairs of eyes in the heads at the both ends. (I-B3b) Weak bipolar head phenotype of trunk fragments. Red arrow indicates that the posterior head has only one eye. (I-B3c) Weak bipolar phenotype of trunk fragments and post-pharyngeal fragments. The white arrowheads indicate that there is not an obvious head at the posterior end. (I-B4) Phenotype of the tail fragment. The head regeneration was inhibited. Scale bars are 300 μ m. (II) Stages of regeneration in bipolar phenotype caused by the GJC inhibitor (heptanol) treatment. The red arrows indicate the eyes at the both ends of worms. The green arrows indicate the bipolar pharynxes. Dorsal view. (II-A1–II-A4) Pre-pharyngeal fragments immediately, 5, 7 and 20 days after cut, respectively. (II-B1–II-B4) Trunk fragments immediately, 5, 7 and 20 days after cut, respectively. Scale bars: II-A1, II-B1—300 μ m; II-A2–II-A4—200 μ m; II-B2–II-B4—300 μ m. (III) Frequency of anteriorized phenotypes. Trunk fragments were exposed to heptanol (strong GJC inhibitor) or hexanol (weak GJC inhibitor) for 2 days and the phenotypes were monitored at 7 days after cutting. Heptanol caused anteriorized phenotypes in 43% of the treated fragments (18% incidence of strong anteriorized phenotype having two heads at the both ends and two pharynxes; 25% incidence of weak anteriorized phenotype having two pharynxes but no head (or Cyclops head) at the posterior end). In contrast, hexanol caused only a very weak anteriorized phenotype (20% incidence). Using the *t* test, the difference between the hexanol and controls was not significant ($P > 0.05$), while the difference between the heptanol and controls was significant ($P < 0.005$).

cases ($n = 423$). The range of anteriorized phenotypes included a loss of tail development, ectopic pharynx posterior to the primary pharynx, appearance of an ectopic eye in the posterior

blastema or a complete head at the posterior end (16% for complete bipolar heads, e.g., Figs. 10I-B2a); such bipolar anterior (janus) animals were fully viable. In contrast, all



worms regenerating in spring water exhibited normal regeneration ($n = 107$). Additional negative controls, in which bipolar head phenotypes were never observed included several thousand worms exposed to a variety of ion channel and pump blockers as part of an electrogenic protein screen in our lab; such reagents, which caused no bipolar phenotype, include blockers of several different kinds of K^+ channels and H^+ pumps (Nogi et al., 2003, 2005). Exposure to hexanol, a reagent similar to heptanol but which is much less effective at blocking GJC than heptanol (Weingart and Bukauskas, 1998), never induced strong anteriorization of the posterior blastema but did inhibit tail regeneration (the weakest class of anteriorization), consistent with a dependence of anteriorization upon the degree of GJC inhibition. Importantly, GJC blockade induced the growth of anterior structures (in many cases, well-formed ectopic heads) and not simply a cessation of regeneration, ruling out toxicity as the mechanism and implicating GJC in events that determine the axial identity of the structure formed during regeneration.

We next sought to ascertain whether the anteriorizing effect was dependent on the AP level from which the fragment originated. Worms were amputated at four levels to make five body fragments: head, prepharyngeal, trunk (including the pharynx), post-pharyngeal and tail fragments (Figs. 10I–A, I–B). To enable quantitative analysis of the effect on regeneration, we defined a simple continuous “anteriorizing index” on which each worm was scored as normal or exhibiting weak/strong/complete anteriorization (see Materials and methods for details). This allowed a direct comparison of the effects observed in each treated group. The data are summarized in Table 1. The phenotypes resulting from the treatments are shown in Fig. 10I, and the time-course of the bipolar head phenotype from the prepharyngeal and trunk fragment is shown in Fig. 10II. The strongest anteriorization due to GJC blockade was observed in the prepharyngeal and trunk fragments (anteriorization indexes of 25.8 and 27.6, respectively). The head and post-pharyngeal fragments were less sensitive (anteriorization indexes of 5.6 and 6.2, respectively). No effect was observed on tail fragments. These data are consistent with the hypothesis that endogenous GJC is involved in the axial patterning along the AP axis during regeneration in the planarian. Our data do not rule out roles for GJC in the dynamic maintenance of pattern in intact worms (Reddien and Alvarado, 2004), and future studies will examine this possibility.

To analyze at a molecular level the patterning changes induced in regenerating worms by GJC closure, we performed whole-mount *in situ* hybridization of marker genes in bipolar worms. The CNS marker *DjPC2* (Agata et al., 1998) was expressed in the brain, VNC and posterior position of the pharynx in the control worms (Fig. 11C). In the bipolar head phenotype worms, *DjPC2* was expressed in the brains at the both ends and two pharynxes that lay asymmetrically as mirror images (Fig. 11K). As determined by *DjPC2* expression, the worms exhibiting a weak bipolar phenotype did not have an obvious brain at the posterior end but did have the V-shaped VNC and the small segment of *DjPC2*-positive cells

(Fig. 11S). The brain marker *Otx* gene, *DjotxB* (Umesono et al., 1999), was expressed in the brain and the cells outlining the posterior half of the mouth in control worms (Fig. 11D). In bipolar head worms, *DjotxB* was expressed in the brains at the both ends and in the mirror imaged-mouths (Fig. 11L). In worms exhibiting a weak bipolar phenotype, *DjotxB* was expressed in the small segment at the posterior end (Fig. 11T), suggesting that the small segment is an incomplete brain.

The innexin gene *inx7* is a good intestine marker (Fig. 3). Normally, the intestine has an asymmetric shape along the AP axis: it has one intestine branch anteriorly connected to the pharynx and two intestine branches posteriorly to the anterior intestine branch (Fig. 11E). In bipolar phenotype worms, the *inx7* expression revealed the symmetric intestine alignment, which has only two intestine branches connected to the two pharynxes in the bipolar head phenotype worms (Fig. 11M) and weak bipolar phenotype worms (Fig. 11U). The tail marker *Hox* gene, *DjAbd-Ba* (Nogi and Watanabe, 2001), was expressed strongly in the tail region posteriorly to the pharynx in the control worms (Fig. 11F). In the bipolar head worms, *DjAbd-Ba* was expressed weakly and broadly in the domain laterally to the pharynxes in the trunk region (Fig. 11N). It was not expressed in the originally-posterior region in the body. In the weak bipolar phenotype worms, *DjAbd-Ba* was expressed in the domain laterally to the pharynxes in the trunk region (Fig. 11V). The expression was much more extensive and stronger than the expression in the severe bipolar head worms. To analyze the patterning changes at an early stage of regeneration, we used *inx3* and *inx13* as early brain markers (Figs. 6C1–C6, D1–D6). In some treated worms, *inx3* and *inx13* were expressed in the small triangle-shaped segment at the posterior end (Figs. 11O, P). At this stage, *inx3* was also expressed in the small pharynx-like spot that was posterior to the original pharynx in the strong phenotype worms (Fig. 11O) and in weak phenotype worms that did not have the *inx3* expression at the posterior end (Fig. 11W).

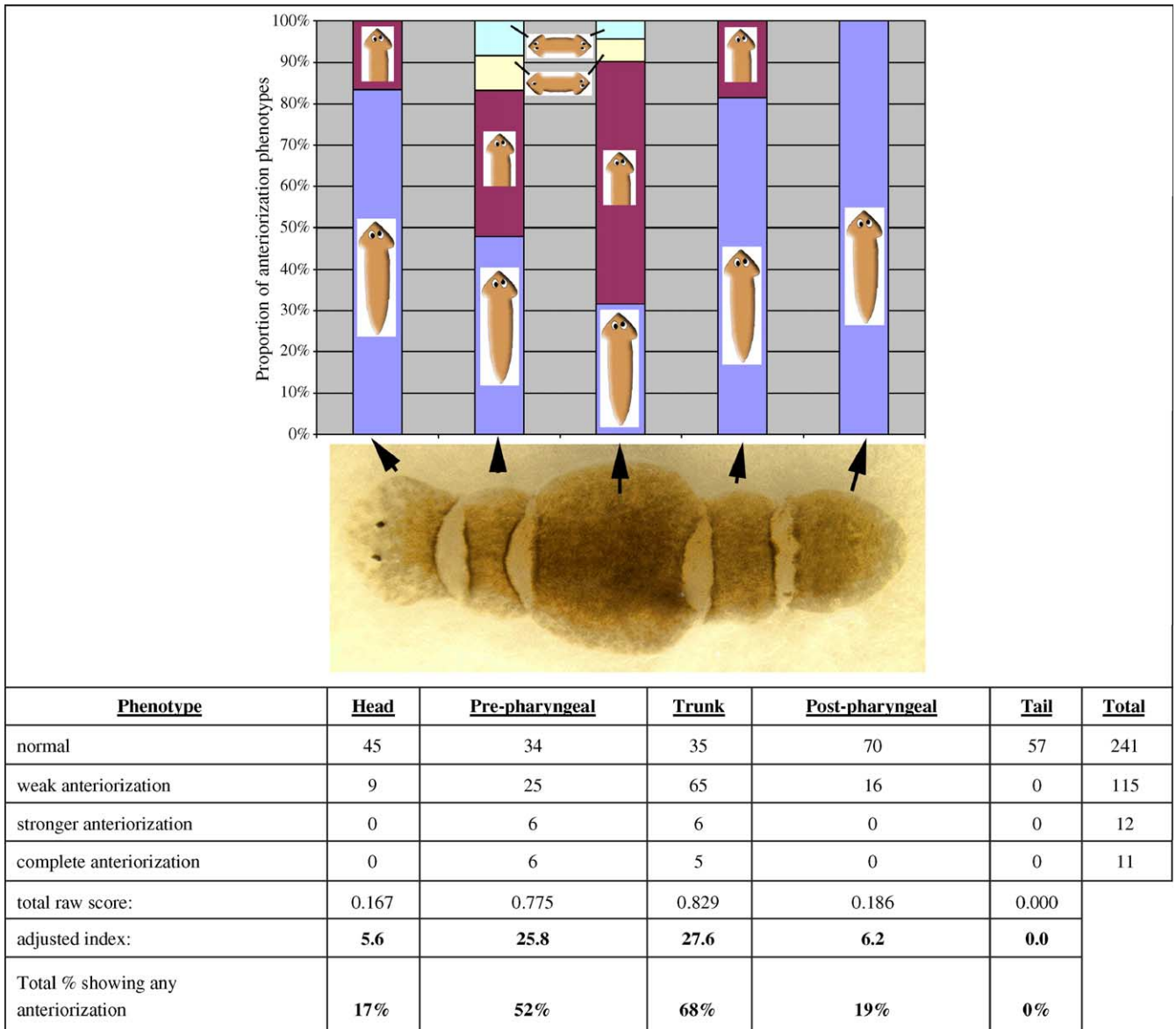
These results demonstrate that the 2-head worms have a bipolar anterior character not only in the outer appearance of the morphology but also in the internal structures, and that the identity of cells (as assayed by marker gene expression) is altered by exposure to a GJC-blocking reagent. Taken together, these data suggest that endogenous GJC is required for the inhibition of anterior character in posterior blastemas during regeneration.

Discussion

Cloning and phylogenetic analysis of innexins

Gap junction-mediated signaling is now known to be involved in a variety of patterning events (Levin, 2001; Lo, 1996). While initially connexins were thought to be the only mediators of GJC, EST and genome projects have recently showed that invertebrates utilize innexin genes to assemble gap junctions, but appear to possess no connexin genes (Bryant, 1997; Phelan and Starich, 2001). Innexins have no significant

Table 1
Dependence of degree of anteriorization on level of cut



Fragments at the levels indicated were exposed to heptanol as described in Materials and methods and assayed for anterior–posterior character of the original fragment’s posterior edge after regeneration. The bar graph illustrates the distribution of regeneration phenotypes while the table’s rows present raw data.

homology to connexins by sequence, but innexin proteins have been shown to form functional gap-junctional channels by direct assays (Dykes et al., 2004; Landesman et al., 1999b; Phelan et al., 1998b). Interestingly, innexin genes were recently found in some vertebrates (Baranova et al., 2004; Panchin et al., 2000) and even viruses (Kroemer and Webb, 2004), suggesting a wide evolutionary conservation of innexin gene family between organisms. In this study, we identified a number of innexin genes (12 cDNA clones and one PCR fragment) from the planarian. Four transmembrane domains, tetrapeptide sequence and the position of cysteine residues are conserved in the amino acid sequences of innexins in all invertebrates reported so far (Dykes et al., 2004; Phelan and Starich, 2001; Potenza et al., 2002, 2003). This key feature is also conserved in the planarian innexins (Fig. 1), consistent

with the hypothesis that the innexin gene family is ubiquitously conserved among animal phyla (Panchin et al., 2000). The total number of innexin genes we found in the planarian is comparable to that in *C. elegans*, which have about 20 innexin genes in their genome (Phelan and Starich, 2001; Starich et al., 2001).

Phylogenetic analysis grouped the planarian innexins into three sets by similarity to *C. elegans* and Lophotrochozoan innexins (Fig. 2). Group I consists of *inx7* and *inx1/G. tigrina panx1*; group II comprises *inx2*, *inx3*, *inx4*, *inx5*, *inx12* and *inx13*; group III contains *inx8*, *inx9*, *inx10* and *inx11*. Interestingly, this analysis and in situ hybridization showed a strict correspondence between grouping according to the sequence phylogeny and that suggested by expression (Figs. 3–9). Group I genes were expressed in the intestine, Group II

genes were expressed in the nervous system (*inx2*, *inx3*, *inx4* and *inx13*) or blastema (*inx5* and *inx12*), and Group III genes were expressed in the parenchyma (*inx8*, *inx9* and *inx11*) or

protonephridia (*inx10*). This is consistent with the existence of at least three innexin genes having the corresponding expression patterns in the ancestral organism of planarians, and a divergence of those ‘prototype’ innexin genes into a family that can potentially provide greater versatility in expression and biological roles in planaria.

The *S. mediterranea* genome contains innexin-like genes similar to our *inx1*–*inx4* and *inx8*–*inx13*. No homologs of *inx5* and *inx6* have been uncovered yet, but it is known to contain at least 3 genes that do not correspond to any of the innexins we characterized in *D. japonica*. It is possible that a homolog of these genes may remain to be discovered in *D. japonica*, which would be an ideal candidate for expression in tissues where prior electron microscopy studies found gap junctions but in which none of our novel innexins were expressed (e.g., secretory cells and muscle; Hori, 1991; Quick and Johnson, 1977).

Expression of innexins in regenerating planaria

Expression of innexins has been observed in the gut, nervous system, visual system and malphigian tubules in *Drosophila* (Bauer et al., 2001, 2002, 2003; Stebbings et al., 2002). Some of those innexin genes were shown to have

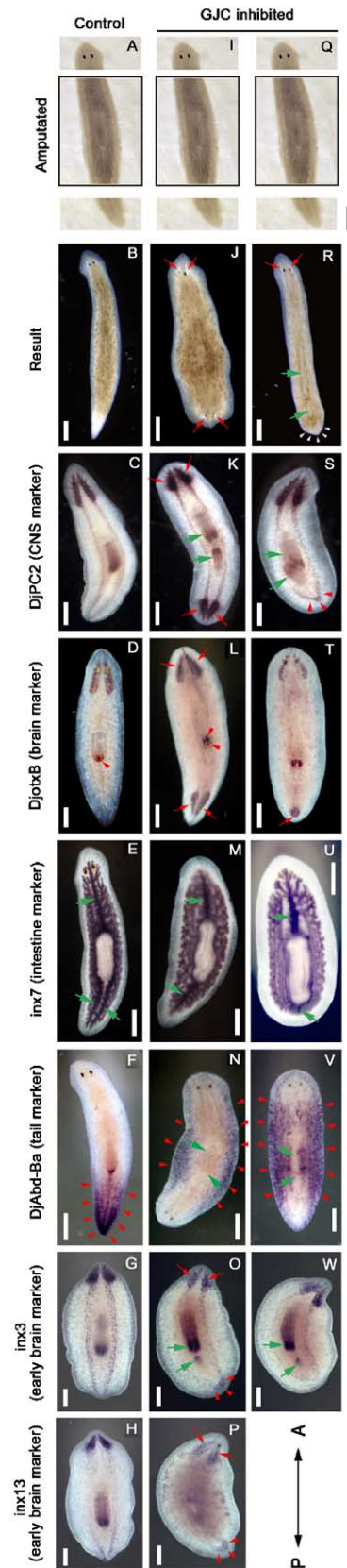


Fig. 11. Marker gene analysis in GJC-inhibited worms during regeneration. Marker gene expression in bipolar phenotype worms generated from trunk worm fragments in which GJC was inhibited by heptanol treatment. (A–H) Control worms. (I–P) Severe bipolar head phenotype having two heads at the both ends and two pharynxes. (Q–W) Weak bipolar phenotype having two pharynxes but no head at the posterior end. (A, I, Q) Immediately after cutting. Dorsal view. (B, J, R) Morphological phenotypes. Red arrows indicate the eyes, and green arrows indicate bipolar pharynxes. White arrowheads indicate that there is no head at the posterior end in panel R. 20 days after cutting. Dorsal view. (C, K, S) Expression of the CNS marker DjPC2. Red arrows indicate that DjPC2 is expressed in the bipolar brain in panel K. The green arrows indicate bipolar pharynxes. The red arrowheads indicate the V-shaped VNC in the posterior end in panel S. 20 days after cutting. Ventral view. (D, L, T) Expression of brain marker DjotxB. The red arrows indicate the brains at the both end in panel L and the small segment expressing DjotxB at the posterior end in panel T. The red arrowheads indicate the expression at the mouths. Note that the mouths are bipolar in panel L. 20 days after cutting. Ventral view. (E, M, U) Expression of the intestine marker *inx7*. The green arrows indicate intestine branches that are asymmetric in panel E and symmetric in panels M and U. 20 days after cutting. Dorsal view in panels E and U. Ventral view in panel M. (F, N, V) Expression of the tail marker DjAbd-Ba. Red arrowheads indicate expression. Note that expression domains are at the regions laterally to the pharynxes but not in the posterior ends in panels N and V. The green arrowheads indicate bipolar pharynxes in panels N and V. Dorsal view in panel F. Ventral view in panels N and V. (G, O, W) Expression of the early brain marker *inx3*. The red arrows indicate the expression in the brain at the anterior end and red arrowheads indicate the small triangle-shaped segment expressing *inx3* at the posterior end in panel O. The green arrows indicate the original pharynx and newly formed pharynx at the posterior region of the original pharynx. Ventral view. Heptanol treatment somewhat slowed regeneration, and in treated worms, early stages were correspondingly observed at 3 days after cutting in panel G. 5 days after cutting (2 days after treatment) in panels O and W. (H, P) Expression of the early brain marker *inx13*. The red arrows indicate expression in the brain at the anterior end and red arrowheads indicate the small triangle-shaped segment expressing *inx13* at the posterior end in panel P. Ventral view. 3 days after cutting in panel H. 5 days after cutting (2 days after treatment) in panel P. In all panels, anterior is to the top. Scale bars: A–F, I–N, Q–V—300 μ m; G–H, O–P, W—250 μ m.

important roles in gut morphogenesis, and neural function in the visual system by mutant analysis (Bauer et al., 2001, 2002; Curtin et al., 2002a,b). Our in situ hybridization data are consistent with the expression and mutant phenotypes of innexin genes in *Drosophila* and also with the expression and function of some connexin genes in vertebrates. For example, connexin genes are expressed in the intestine, nervous system, visual system (lens and retina) and kidney in vertebrates (Cook and Becker, 1995; Goodenough, 1992; Haefliger et al., 2004; Rozental et al., 2000; Umino and Saito, 2002; Wang and Daniel, 2001).

While all Group II innexins are expressed in the brain, the individual distribution patterns differ (Figs. 4 and 6), resembling the differential innexin gene expression in the CNS in the leech and rat (Bruzzone et al., 2003; Dykes et al., 2004). *inx2*, *inx3* and *inx13* are expressed in both the medial and lateral region. *Inx4* is, however, not expressed in the lateral region, but only in the medial region at early stages in the regenerating brain. The expression of *inx3* and *inx13* is initiated in the regenerating brain at only 1 day after cutting, making homotypic and heterotypic junctions available at early stages of brain regeneration (Dykes et al., 2004; Yeager et al., 1998).

Only *inx4* is expressed in the photoreceptor cells (Fig. 5), initiating at 4 days after cutting. This is significantly later than the expression of the photoreceptor genes (*Djeyea* and *Djsix-1*, transcription factors required for the eye morphogenesis, which are detected at 2 days after cutting, and the opsin gene *Djops*, initiating at 3 days after cutting; Mannini et al., 2004). *inx4* is also expressed in the medial region of the brain (Figs. 6B2–B6), to which the photoreceptor cells project (Sakai et al., 2000). Taken together, these observations make a physiological role in transmitting visual information more likely rather than early roles in eye regeneration for *inx4*. Consistently, the innexin genes, *shaking-B* and *ogre*, have important roles in visual system function in adult *Drosophila* (Curtin et al., 2002b).

inx10 was expressed in the protonephridia (Fig. 9). The protonephridia is a primitive excretory system in invertebrates, which is consisted from tubule cells and ciliated flame cells (Hyman, 1951). Although we cannot be certain that the cells expressing *inx10* are 100% identical to all of the protonephridia cells, their distribution in whole-mount and plastic sections is very similar to the classical distribution revealed by electron microscopy (Kishida, 1979). Consistently, nine connexins are expressed in the vertebrate kidney as well (Haefliger et al., 2004; Silverstein et al., 2003).

Previous electron microscopy studies found intercellular gap junctions between migrating regenerative cells and stationary parenchyma cells ('fixed parenchyma cells') in early blastemas. Fixed parenchyma cells are abundant and possess long and slender cytoplasmic processes which connect with each other and fill the narrow spaces among regenerative cells in the blastemas (Hori, 1991), leading to the suggestion that the blastema-specific heterotypic GJC has a functional role in planarian regeneration (Hori, 1991). Our expression data for Group III genes are consistent with prior electron

microscopy observations. *inx5* is expressed in the anterior blastema and *inx12* is expressed in both of the anterior and posterior blastemas; *inx8*, *inx9* and *inx11* are expressed differentially in the parenchyma cells. It is not yet known whether the blastema innexin genes (*inx5* and *inx12*) are expressed in the regenerative cells and whether the parenchyma innexin genes (*inx8*, *inx9* and *inx11*) are expressed in the fixed parenchyma cells. Determining the cell types using immuno-electron microscopy and testing the possibility of heterotypic gap-junctional channels between the blastema innexins and parenchyma innexins represent important future areas for work to help understand the involvement of the blastema-specific gap-junctional communication in the planarian regeneration.

Our results provide a possible explanation for the classical observation (Rustia, 1924) that HCl exposure induces a bipolar anterior phenotype. Since acidification rapidly inhibits innexin-based GJC (Landesman et al., 1999a), HCl could induce anteriorization if it acidified the intracellular milieu and blocked gap junctions through a pH-dependent mechanism. Our data are also consistent with the finding that colchicine exposure induces a bipolar head phenotype; the finding that colchicine treatment caused detachment of the cytoplasmic processes of the fixed parenchyma cells from the regenerative cells in the blastema and caused separation of gap junctions between the 2 types of cells (Hori, 1991) specifically suggests *inx9* and *inx12* as good candidates for future functional studies of the roles of heterologous gap junctions between parenchyma cells and regenerative cells in AP patterning.

The presence of *inx5* and *inx12* in the blastema is consistent with GJC-dependent mechanisms operating locally within the regenerating tissues. One possible role is within the planarian stem cells (neoblasts). *Drosophila inx4* is expressed in the germ stem cells and is required for differentiation (Gilboa et al., 2003; Gilboa and Lehmann, 2004). Similarly, Connexin43 is expressed in neural progenitor cells and has an important role for their proliferation and survival (Cheng et al., 2004), and a number of recent studies have identified specific gap-junctional properties in mammalian stem cells (Cai et al., 2004; Tazuke et al., 2002; Trosko et al., 2000; Wong et al., 2004). The blastema innexins may participate in proposed roles of gap junctions for maintenance of multipotency and differentiation of stem cells (Tazuke et al., 2002; Trosko et al., 2000).

In contrast, other innexins (*inx8*, *inx9* and *inx11*) form long-range paths that could potentially underlie long-range communication between the anterior and posterior regions (Kobayashi et al., 1999a,b; Nogi and Watanabe, 2001), analogously to the obligate GJC which exists between the left and right sides during vertebrate laterality determination (Levin and Mercola, 1998, 1999). Ascertaining the roles of individual innexins in regeneration will require extensive combinatorial RNAi experiments (to overcome redundancy and probe roles of heterotypic/heteromeric gap junctions). Importantly, our data suggest that the effect of GJC inhibition is not entirely localized to the blastema since molecular marker analysis revealed a rearrangement of anterior and posterior expression domains (Fig. 11); while ectopic head structures expressed anterior markers, tail

marker expression was shut off in the posterior blastemas, but was up-regulated in lateral tissues. These observations indicate that GJC is required for the establishment of identity throughout the animal, including cells in regions that are not undergoing regeneration (such as lateral cells, Figs. 11N, V).

GJC is involved in determination of anterior–posterior identity during regeneration

Heptanol is a potent reagent that blocks both electrical and chemical coupling in invertebrate gap junctions (Adler and Woodruff, 2000; Anderson and Woodruff, 2001; Brooks and Woodruff, 2004; Bukauskas et al., 1992; Carrow and Levitan, 1989; Mire et al., 2000; Peracchia, 1991; Weingart and Bukauskas, 1998). Heptanol causes a well-characterized, rapid and reversible inhibition of GJC (Deleze and Herve, 1983; Spray and Burt, 1990), and recent studies make a strong case for selective action on GJC when used below 1 mM (Christ et al., 1999; Garcia-Dorado et al., 1997), orders of magnitude above the dose we utilized. Worms exposed to heptanol during the first 2 days of regeneration exhibited significant anteriorization, ranging from an inhibition of tail development to the appearance of a complete second head at the posterior blastema. This treatment did not induce a disruption of regeneration per se (as head structures regenerated normally), nor did it result in general toxicity. The penetrance of the effect was at about 57% (Fig. 10III), which is similar to that obtained in GJC and ion flux inhibitor experiments in both vertebrates and invertebrates (Levin and Mercola, 1998; Levin et al., 2002); why not all of the worms were affected is not known, but may reflect differential susceptibility of the individual worms due to cryptic genetic or environmental factors during their life-span. We did not observe anteriorized phenotypes in hundreds of planaria tested with a panel of drugs targeting other ion flux regulators (Nogi et al., 2003, 2005). These data suggest that assignment of posterior fate during regeneration is GJC-dependent. Our data do not rule out additional possible roles for GJC, since more subtle phenotypes may not have been detected by our assay focusing on anterior–posterior polarity.

The fate of posterior blastemas was changed to an anteriorized identity by GJC inhibitors. This coherent change of large-scale morphology, as distinct from simple inhibition of growth, results suggests that GJC is not just a permissive physiological housekeeping mechanism but rather serves to transduce non-cell-autonomous signals instructive with respect to anterior–posterior identity during regeneration (Armstrong and Armstrong, 1990; Duband et al., 1990; Gilbert, 1991; Gilbert and Saxén, 1993; Lee et al., 2004). Since heptanol is very volatile and is rapidly-reversible in innexin-based gap-junction preparations (Landesman et al., 1999a), this process is likely to occur during the first 48 h of regeneration, although persistent effects cannot be ruled out. We are currently pursuing investigations into the behavior of the resulting 2-headed worms; these represent a unique opportunity for insights into the integration of neural control mechanisms, as no other model system offers viable true bipolar anterior animals.

We observed that the prepharyngeal and trunk fragments were most likely to anteriorize following GJC inhibition (Fig. 10), while the head fragment was resistant. It is possible that our abrogation of GJC was less than total (dosages were indeed chosen to avoid general toxicity from loss of other important GJC functions), and that a complete inhibition of GJC would anteriorize even the posterior blastema of the head fragment. The relative resistance of the head fragment is consistent with models positing that the distal anterior cells are sources of head determinants. The planarian noggin-like gene, *Djnlg*, is expressed in both the anterior and posterior blastemas at 1 day after cutting, and is restricted to the anterior blastema by the second day (Ogawa et al., 2002). This dynamic transition of *Djnlg* expression from symmetric to asymmetric along the AP axis may suggest that head regeneration is a default fate in regeneration blastemas, and that head regeneration is suppressed in the posterior blastema at 2 days after cutting. This is consistent with GJC-based long-range transfer of as yet uncharacterized signaling molecules such as head inhibitors, and provides a molecular candidate mechanism to explain classical results (Wolff, 1962) positing the existence of a gradient of substances inhibiting the generation of anterior structures in the posterior region of the original worm.

The dependence of GJC blocker effect upon the level of origin of the fragment indicates that medial and edge tissues are already different and possess some knowledge of their AP position when cut. Indeed, this might reflect the existence and dependence of GJC-dependent flows of endogenous head inhibitor gradient(s) from the anterior to posterior region. Importantly, in contrast to previous work focused on identifying proteins functioning in long-range gradients of planarian head inhibitors (Lange and Steele, 1978), our data suggest the involvement of as yet unidentified small molecule signals in this role. Our data suggest that, similar to the involvement of the GJC in left–right patterning in vertebrates (Levin and Mercola, 1998, 1999), innexin-based GJC does not originate anterior–posterior information de novo, but rather is a conduit for its transmission to distal tissues.

Taken together, our functional and expression data suggest the presence of a deep conservation of GJC-based signaling mechanisms in large-scale axial patterning among vertebrates and invertebrates, despite different molecular bases for the GJC-mediating structures involved. Future efforts aimed at understanding the molecular identity of the GJC-permeable signals that dictate AP character will greatly enrich the understanding of patterning in regeneration and lead to biomedically-relevant gain-of-function approaches.

Acknowledgments

We thank Nestor J. Oviedo for helpful discussions regarding these data, Ricardo Zayas and Phillip A. Newmark for kindly sharing the unpublished sequences of innexin-like clones in the sexual *S. mediterranea* EST database, Dayong Qiu for histology, and the National Science Foundation for supporting this work (NSF CAREER grant IBN #0347295). This investigation was conducted in a Forsyth Institute facility

renovated with support from Research Facilities Improvement Grant Number CO6RR11244 from the National Center for Research Resources, National Institutes of Health.

References

- Adler, E.L., Woodruff, R.I., 2000. Varied effects of 1-octanol on gap junctional communication between ovarian epithelial cells and oocytes of *Oncopeltus fasciatus*, *Hyalophora cecropia*, and *Drosophila melanogaster*. *Arch. Insect Biochem. Physiol.* 43, 22–32.
- Agata, K., Soejima, Y., Kato, K., Kobayashi, C., Umesono, Y., Watanabe, K., 1998. Structure of the planarian central nervous system (CNS) revealed by neuronal cell markers. *Zool. Sci.* 15, 433–440.
- Allen, F., Tickle, C., Warner, A., 1990. The role of gap junctions in patterning of the chick limb bud. *Development* 108, 623–634.
- Alvarado, A.S., Newmark, P.A., 1998. The use of planarians to dissect the molecular basis of metazoan regeneration. *Wound Repair Regen.* 6, 413–420.
- Alvarado, A.S., Newmark, P.A., Robb, S.M., Juste, R., 2002. The *Schmidtea mediterranea* database as a molecular resource for studying plathyhelminthes, stem cells and regeneration. *Development* 129, 5659–5665.
- Anderson, K.L., Woodruff, R.I., 2001. A gap junctionally transmitted epithelial cell signal regulates endocytic yolk uptake in *Oncopeltus fasciatus*. *Dev. Biol.* 239, 68–78.
- Armstrong, P.B., Armstrong, M.T., 1990. An instructive role for the interstitial matrix in tissue patterning: tissue segregation and intercellular invasion. *J. Cell Biol.* 110, 1439–1455.
- Baranova, A., Ivanov, D., Petrash, N., Pestova, A., Skoblov, M., Kelmanson, I., Shagin, D., Nazarenko, S., Geraymovych, E., Litvin, O., Tiunova, A., Born, T.L., Usman, N., Staroverov, D., Lukyanov, S., Panchin, Y., 2004. The mammalian pannexin family is homologous to the invertebrate innexin gap junction proteins. *Genomics* 83, 706–716.
- Bauer, R., Lehmann, C., Hoch, M., 2001. Gastrointestinal development in the *Drosophila* embryo requires the activity of innexin gap junction channel proteins. *Cell Adhes. Commun.* 8, 307–310.
- Bauer, R., Lehmann, C., Fuss, B., Eckardt, F., Hoch, M., 2002. The *Drosophila* gap junction channel gene innexin 2 controls foregut development in response to Wingless signalling. *J. Cell Sci.* 115, 1859–1867.
- Bauer, R., Martini, J., Lehmann, C., Hoch, M., 2003. Cellular distribution of innexin 1 and 2 gap junctional channel proteins in epithelia of the *Drosophila* embryo. *Cell Adhes. Commun.* 10, 221–225.
- Brooks, R.A., Woodruff, R.I., 2004. Calmodulin transmitted through gap junctions stimulates endocytic incorporation of yolk precursors in insect oocytes. *Dev. Biol.* 271, 339–349.
- Bruzzone, R., Hormuzdi, S.G., Barbe, M.T., Herb, A., Monyer, H., 2003. Pannexins, a family of gap junction proteins expressed in brain. *Proc. Natl. Acad. Sci. U. S. A.* 100, 13644–13649.
- Bryant, P.J., 1997. Junction genetics. *Dev. Genet.* 20, 75–90.
- Budd, S., Lipton, S., 1998. Calcium tsunamis. *Nat. Neurosci.* 1, 431–432.
- Bukauskas, F., Kempf, C., Weingart, R., 1992. Electrical coupling between cells of the insect *Aedes albopictus*. *J. Physiol.* 448, 321–337.
- Cai, J., Cheng, A., Luo, Y., Lu, C., Mattson, M.P., Rao, M.S., Furukawa, K., 2004. Membrane properties of rat embryonic multipotent neural stem cells. *J. Neurochem.* 88, 212–226.
- Carrow, G.M., Levitan, I.B., 1989. Selective formation and modulation of electrical synapses between cultured Aplysia neurons. *J. Neurosci.* 9, 3657–3664.
- Cebria, F., Kudome, T., Nakazawa, M., Mineta, K., Ikeo, K., Gojobori, T., Agata, K., 2002. The expression of neural-specific genes reveals the structural and molecular complexity of the planarian central nervous system. *Mech. Dev.* 116, 199–204.
- Chanson, M., Bruzzone, R., Bosco, D., Meda, P., 1989. Effects of n-alcohols on junctional coupling and amylase secretion of pancreatic acinar cells. *J. Cell. Physiol.* 139, 147–156.
- Cheng, A., Tang, H., Cai, J., Zhu, M., Zhang, X., Rao, M., Mattson, M.P., 2004. Gap junctional communication is required to maintain mouse cortical neural progenitor cells in a proliferative state. *Dev. Biol.* 272, 203–216.
- Christ, G.J., Spektor, M., Brink, P.R., Barr, L., 1999. Further evidence for the selective disruption of intercellular communication by heptanol. *Am. J. Physiol.* 276, H1911–H1917.
- Coelho, C.N., Kosher, R.A., 1991. A gradient of gap junctional communication along the anterior–posterior axis of the developing chick limb bud. *Dev. Biol.* 148, 529–535.
- Cook, J.E., Becker, D.L., 1995. Gap junctions in the vertebrate retina. *Microsc. Res. Tech.* 31, 408–419.
- Corpet, F., 1988. Multiple sequence alignment with hierarchical clustering. *Nucleic Acids Res.* 16, 10881–10890.
- Crompton, D., Todman, M., Wilkin, M., Ji, S., Davies, J., 1995. Essential and neural transcripts from the *Drosophila* shaking-B locus are differentially expressed in the embryonic mesoderm and pupal nervous system. *Dev. Biol.* 170, 142–158.
- Curtin, K.D., Zhang, Z., Wyman, R.J., 2002a. Gap junction proteins are not interchangeable in development of neural function in the *Drosophila* visual system. *J. Cell Sci.* 115, 3379–3388.
- Curtin, K.D., Zhang, Z., Wyman, R.J., 2002b. Gap junction proteins expressed during development are required for adult neural function in the *Drosophila* optic lamina. *J. Neurosci.* 22, 7088–7096.
- Deleze, J., Herve, J.C., 1983. Effect of several uncouplers of cell-to-cell communication on gap junction morphology in mammalian heart. *J. Membr. Biol.* 74, 203–215.
- Duband, J.L., Dufour, S., Thiery, J.P., 1990. The instructive role of fibronectins in cell migrations during embryonic development. *Ann. N. Y. Acad. Sci.* 588, 273–280.
- Dykes, I.M., Freeman, F.M., Bacon, J.P., Davies, J.A., 2004. Molecular basis of gap junctional communication in the CNS of the leech *Hirudo medicinalis*. *J. Neurosci.* 24, 886–894.
- Ewart, J.L., Cohen, M.F., Meyer, R.A., Huang, G.Y., Wessels, A., Gourdie, R.G., Chin, A.J., Park, S.M.J., Lazatin, B.O., Villabon, S., Lo, C.W., 1997. Heart and neural tube defects in transgenic mice overexpressing the Cx43 gap junction gene. *Development* 124, 1281–1292.
- Falk, M.M., 2000. Biosynthesis and structural composition of gap junction intercellular membrane channels. *Eur. J. Cell Biol.* 79, 564–574.
- Fraser, S.E., Green, C.R., Bode, H.R., Gilula, N.B., 1987. Selective disruption of gap junctional communication interferes with a patterning process in hydra. *Science* 237, 49–55.
- Garcia-Dorado, D., Inserte, J., Ruiz-Meana, M., Gonzalez, M.A., Solares, J., Julia, M., Barrabes, J.A., Soler-Soler, J., 1997. Gap junction uncoupler heptanol prevents cell-to-cell progression of hypercontracture and limits necrosis during myocardial reperfusion. *Circulation* 96, 3579–3586.
- Germain, G., Ancil, M., 1996. Evidence for intercellular coupling and connexin-like protein in the luminescent endoderm of *Renilla koellikeri* (Cnidaria Anthozoa). *Biol. Bull.* 191, 353–366.
- Gilbert, S.F., 1991. *Developmental Biology*. Sinauer Associates, Sunderland, MA.
- Gilbert, S.F., Saxén, L., 1993. Spemann's organizer: models and molecules. *Mech. Dev.* 41, 73–89.
- Gilboa, L., Lehmann, R., 2004. How different is Venus from Mars? The genetics of germ-line stem cells in *Drosophila* females and males. *Development* 131, 4895–4905.
- Gilboa, L., Forbes, A., Tazuke, S.I., Fuller, M.T., Lehmann, R., 2003. Germ line stem cell differentiation in *Drosophila* requires gap junctions and proceeds via an intermediate state. *Development* 130, 6625–6634.
- Goodenough, D.A., 1992. The crystalline lens. A system networked by gap junctional intercellular communication. *Semin. Cell Biol.* 3, 49–58.
- Goodenough, D.A., Goliger, J.A., Paul, D.L., 1996. Connexins, connexons, and intercellular communication. *Annu. Rev. Biochem.* 65, 475–502.
- Haefliger, J.A., Nicod, P., Meda, P., 2004. Contribution of connexins to the function of the vascular wall. *Cardiovasc. Res.* 62, 345–356.
- Hori, I., 1991. Role of fixed parenchyma cells in blastema formation of the planarian *Dugesia japonica*. *Int. J. Dev. Biol.* 35, 101–108.
- Hyman, L.H., 1951. *The Invertebrates: Platyhelminthes and Rhynchocoela*. McGraw-Hill Book Co, London.
- Ishii, S., 1980. The ultrastructure of the protonephridial flame cell of the freshwater planarian *Bdellocephala brunnea*. *Cell Tissue Res.* 206, 441–449.

- Kimura, H., Oyamada, Y., Ohshika, H., Mori, M., Oyamada, M., 1995. Reversible inhibition of gap junctional intercellular communication, synchronous contraction, and synchronism of intracellular Ca²⁺ fluctuation in cultured neonatal rat cardiac myocytes by heptanol. *Exp. Cell Res.* 220, 348–356.
- Kishida, Y., 1979. Morphology in regeneration of a freshwater planarian, *Dugesia japonica japonica*. *Bull. Sch. Educ., Okayama Univ.* 52, 1–9.
- Kobayashi, C., Nogi, T., Watanabe, K., Agata, K., 1999a. Ectopic pharynxes arise by regional reorganization after anterior/posterior chimera in planarians. *Mech. Dev.* 89, 25–34.
- Kobayashi, C., Watanabe, K., Agata, K., 1999b. The process of pharynx regeneration in planarians. *Dev. Biol.* 211, 27–38.
- Kroemer, J.A., Webb, B.A., 2004. Polydnavirus genes and genomes: emerging gene families and new insights into polydnavirus replication. *Annu. Rev. Entomol.* 49, 431–456.
- Krutovskikh, V., Yamasaki, H., 1997. The role of gap junctional intercellular communication (GJIC) disorders in experimental and human carcinogenesis. *Histol. Histopathol.* 12, 761–768.
- Krutovskikh, V., Yamasaki, H., 2000. Connexin gene mutations in human genetic diseases. *Mutat. Res.* 462, 197–207.
- Landesman, Y., White, T.W., Starich, T.A., Shaw, J.E., Goodenough, D.A., Paul, D.L., 1999a. Innexin-3 forms connexin-like intercellular channels. *J. Cell Sci.* 112, 2391–2396.
- Landesman, Y., White, T.W., Starich, T.A., Shaw, J.E., Goodenough, D.A., Paul, D.L., 1999b. Innexin-3 forms connexin-like intercellular channels. *J. Cell Sci.* 112 (Pt. 14), 2391–2396.
- Lange, C.S., Steele, V.E., 1978. The mechanism of anterior–posterior polarity control in planarians. *Differentiation* 11, 1–12.
- Lee, H.Y., Kleber, M., Hari, L., Brault, V., Suter, U., Taketo, M.M., Kemler, R., Sommer, L., 2004. Instructive role of Wnt/beta-catenin in sensory fate specification in neural crest stem cells. *Science* 303, 1020–1023.
- Levin, M., 2001. Isolation and community: the role of gap junctional communication in embryonic patterning. *J. Membr. Biol.* 185, 177–192.
- Levin, M., Mercola, M., 1998. Gap junctions are involved in the early generation of left right asymmetry. *Dev. Biol.* 203, 90–105.
- Levin, M., Mercola, M., 1999. Gap junction-mediated transfer of left–right patterning signals in the early chick blastoderm is upstream of Shh asymmetry in the node. *Development* 126, 4703–4714.
- Levin, M., Mercola, M., 2000. Expression of connexin 30 in *Xenopus* embryos and its involvement in hatching gland function. *Dev. Dyn.* 219, 96–101.
- Levin, M., Thorlin, T., Robinson, K.R., Nogi, T., Mercola, M., 2002. Asymmetries in H⁺/K⁺-ATPase and cell membrane potentials comprise a very early step in left–right patterning. *Cell* 111, 77–89.
- Lo, C.W., 1996. The role of gap junction membrane channels in development. *J. Bioenerg. Biomembr.* 28, 379–385.
- Lo, C.W., Waldo, K.L., Kirby, M.L., 1999. Gap junction communication and the modulation of cardiac neural crest cells. *Trends Cardiovasc. Med.* 9, 63–69.
- Makarenkova, H., Patel, K., 1999. Gap junction signalling mediated through Connexin-43 is required for chick limb development. *Dev. Biol.* 207, 380–392.
- Makarenkova, H., Becker, D.L., Tickle, C., Warner, A.E., 1997. Fibroblast growth factor 4 directs gap junction expression in the mesenchyme of the vertebrate limb. *Bud. J. Cell Biol.* 138, 1125–1137.
- Mannini, L., Rossi, L., Deri, P., Gremigni, V., Salvetti, A., Salo, E., Batistoni, R., 2004. Djeyes absent (Djeya) controls prototypic planarian eye regeneration by cooperating with the transcription factor Djsix-1. *Dev. Biol.* 269, 346–359.
- Meda, P., 1996. The role of gap junction membrane channels in secretion and hormonal action. *J. Bioenerg. Biomembr.* 28, 369–377.
- Mineta, K., Nakazawa, M., Cebria, F., Ikeo, K., Agata, K., Gojobori, T., 2003. Origin and evolutionary process of the CNS elucidated by comparative genomics analysis of planarian ESTs. *Proc. Natl. Acad. Sci. U. S. A.* 100, 7666–7671.
- Mire, P., Nasse, J., Venable-Thibodeaux, S., 2000. Gap junctional communication in the vibration-sensitive response of sea anemones. *Hear Res.* 144, 109–123.
- Morgan, T., 1901. *Regeneration*. Macmillan, New York.
- Newmark, P.A., Alvarado, A.S., 2002. Not your father's planarian: a classic model enters the era of functional genomics. *Nat. Rev., Genet.* 3, 210–219.
- Nogi, T., Watanabe, K., 2001. Position-specific and non-colinear expression of the planarian posterior (Abdominal-B-like) gene. *Dev. Growth Differ.* 43, 177–184.
- Nogi, T., Adams, D.S., Levin, M., 2003. Electric controls of regeneration in planaria. *Dev. Biol.* 259, 586.
- Nogi, T., Yuan, Y.E., Sorocco, D., Perez-Tomas, R., Levin, M., 2005. Eye regeneration assay reveals an invariant functional left–right asymmetry in the early bilaterian, *Dugesia japonica*. *Lateralitas* 10, 193–205.
- Ogawa, K., Ishihara, S., Saito, Y., Mineta, K., Nakazawa, M., Ikeo, K., Gojobori, T., Watanabe, K., Agata, K., 2002. Induction of a noggin-like gene by ectopic DV interaction during planarian regeneration. *Dev. Biol.* 250, 59–70.
- Omori, Y., Dufrot-Dancer, A., Mesnil, M., Yamasaki, H., 1998. Role of connexin (gap junction) genes in cell growth control. *Toxicol. Lett.* 96–97, 105–110.
- Omori, Y., Zaidan Dagli, M.L., Yamakage, K., Yamasaki, H., 2001. Involvement of gap junctions in tumor suppression: analysis of genetically-manipulated mice. *Mutat. Res.* 477, 191–196.
- Panchin, Y., Kelmanson, I., Matz, M., Lukyanov, K., Usman, N., Lukyanov, S., 2000. A ubiquitous family of putative gap junction molecules. *Curr. Biol.* 10, R473–R474.
- Peracchia, C., 1991. Effects of the anesthetics heptanol, halothane and isoflurane on gap junction conductance in crayfish septate axons: a calcium- and hydrogen-independent phenomenon potentiated by caffeine and theophylline, and inhibited by 4-aminopyridine. *J. Membr. Biol.* 121, 67–78.
- Phelan, P., Starich, T.A., 2001. Innexins get into the gap. *BioEssays* 23, 388–396.
- Phelan, P., Bacon, J.P., Davies, J.A., Stebbings, L.A., Todman, M.G., Avery, L., Baines, R.A., Barnes, T.M., Ford, C., Hekimi, S., Lee, R., Shaw, J.E., Starich, T.A., Curtin, K.D., Sun, Y.A., Wyman, R.J., 1998a. Innexins: a family of invertebrate gap-junction proteins. *Trends Genet.* 14, 348–349.
- Phelan, P., Stebbings, L.A., Baines, R.A., Bacon, J.P., Davies, J.A., Ford, C., 1998b. *Drosophila* Shaking-B protein forms gap junctions in paired *Xenopus* oocytes. *Nature* 391, 181–184.
- Potenza, N., del Gaudio, R., Rivieccio, L., Russo, G.M., Geraci, G., 2002. Cloning and molecular characterization of the first innexin of the phylum annelida—Expression of the gene during development. *J. Mol. Evol.* 54, 312–321.
- Potenza, N., del Gaudio, R., Chiusano, M.L., Russo, G.M., Geraci, G., 2003. Specificity of cellular expression of *C. variopedatus* polychaete innexin in the developing embryo: evolutionary aspects of innexins' heterogeneous gene structures. *J. Mol. Evol.* 57 (Suppl 1), S165–S173.
- Quick, D.C., Johnson, R.G., 1977. Gap junctions and rhombic particle arrays in planaria. *J. Ultrastruct. Res.* 60, 348–361.
- Reddien, P.W., Alvarado, A.S., 2004. Fundamentals of planarian regeneration. *Annu. Rev. Cell Dev. Biol.* 20, 725–757.
- Reddien, P.W., Bermange, A.L., Murfitt, K.J., Jennings, J.R., Sanchez Alvarado, A., 2005. Identification of genes needed for regeneration, stem cell function, and tissue homeostasis by systematic gene perturbation in planaria. *Dev. Cell* 8, 635–649.
- Rozental, R., Srinivas, M., Gokhan, S., Urban, M., Dermietzel, R., Kessler, J.A., Spray, D.C., Mehler, M.F., 2000. Temporal expression of neuronal connexins during hippocampal ontogeny. *Brain Res. Brain Res. Rev.* 32, 57–71.
- Rustia, C., 1924. The control of biaxial development in the reconstitution of pieces of planaria. *J. Exp. Zool.* 42, 111–142.
- Sakai, T., Agata, K., Orii, H., Watanabe, K., 2000. Organization and regeneration ability of spontaneous supernumerary eyes in planarians 'eye regeneration field and pathway selection by optic nerves'. *Zool. Sci.* 17, 375–381.
- Severs, N.J., 1999. Cardiovascular disease. *Novartis Found. Symp.* 219, 188–206.
- Silverstein, D.M., Thornhill, B.A., Leung, J.C., Vehaskari, V.M., Craver, R.D.,

- Trachtman, H.A., Chevalier, R.L., 2003. Expression of connexins in the normal and obstructed developing kidney. *Pediatr. Nephrol.* 18, 216–224.
- Spray, D.C., Burt, J.M., 1990. Structure-activity relations of the cardiac gap junction channel. *Am. J. Physiol.* 258, C195–C205.
- Starich, T.A., Lee, R.Y., Panzarella, C., Avery, L., Shaw, J.E., 1996. *eat-5* and *unc-7* represent a multigene family in *Caenorhabditis elegans* involved in cell–cell coupling. *J. Cell Biol.* 134, 537–548.
- Starich, T., Sheehan, M., Jadrich, J., Shaw, J., 2001. Innexins in *C. elegans*. *Cell Adhes. Commun.* 8, 311–314.
- Stebbins, L.A., Todman, M.G., Phelan, P., Bacon, J.P., Davies, J.A., 2000. Two *Drosophila* innexins are expressed in overlapping domains and cooperate to form gap-junction channels. *Mol. Biol. Cell* 11, 2459–2470.
- Stebbins, L.A., Todman, M.G., Phillips, R., Greer, C.E., Tam, J., Phelan, P., Jacobs, K., Bacon, J.P., Davies, J.A., 2002. Gap junctions in *Drosophila*: developmental expression of the entire innexin gene family. *Mech. Dev.* 113, 197–205.
- Tazuke, S.I., Schulz, C., Gilboa, L., Fogarty, M., Mahowald, A.P., Guichet, A., Ephrussi, A., Wood, C.G., Lehmann, R., Fuller, M.T., 2002. A germline-specific gap junction protein required for survival of differentiating early germ cells. *Development* 129, 2529–2539.
- Trosko, J., Chang, C., Wilson, M., Upham, B., Hayashi, T., Wade, M., 2000. Gap junctions and the regulation of cellular functions of stem cells during development and differentiation. *Methods* 20, 245–264.
- Umesono, Y., Watanabe, K., Agata, K., 1999. Distinct structural domains in the planarian brain defined by the expression of evolutionarily conserved homeobox genes. *Dev. Genes Evol.* 209, 31–39.
- Umino, Y., Saito, T., 2002. Spatial and temporal patterns of distribution of the gap junctional protein connexin43 during retinal regeneration of adult newt. *J. Comp. Neurol.* 454, 255–262.
- Wakeford, R.J., 1979. Cell contact and positional communication in hydra. *J. Embryol. Exp. Morphol.* 54, 171–183.
- Wang, Y.F., Daniel, E.E., 2001. Gap junctions in gastrointestinal muscle contain multiple connexins. *Am. J. Physiol.: Gastrointest. Liver Physiol.* 281, G533–G543.
- Warner, A., 1999. Interactions between growth factors and gap junctional communication in developing systems. *Novartis Found. Symp.* 219, 60–72.
- Watanabe, K., Sakai, F., Orii, H., 1997. Stepwise dilution screening of a cDNA library by polymerase chain reaction. *Anal. Biochem.* 252, 213–214.
- Weingart, R., Bukauskas, F.F., 1998. Long-chain *n*-alkanols and arachidonic acid interfere with the Vm-sensitive gating mechanism of gap junction channels. *Pflugers Arch.* 435, 310–319.
- Wolff, E., 1962. Recent researches on the regeneration of planaria. In: Rudnick, D. (Ed.), *Regeneration: 20th Growth Symposium*. The Ronald Press, New York, pp. 53–84.
- Wong, R.C., Pebay, A., Nguyen, L.T., Koh, K.L., Pera, M.F., 2004. Presence of functional gap junctions in human embryonic stem cells. *Stem Cells* 22, 883–889.
- Yazaki, I., Dale, B., Tosti, E., 1999. Functional gap junctions in the early sea urchin embryo are localized to the vegetal pole. *Dev. Biol.* 212, 503–510.
- Yeager, M., Unger, V.M., Falk, M.M., 1998. Synthesis, assembly and structure of gap junction intercellular channels. *Curr. Opin. Struct. Biol.* 8, 517–524.
- Zhang, Z., Curtin, K.D., Sun, Y.A., Wyman, R.J., 1999. Nested transcripts of gap junction gene have distinct expression patterns. *J. Neurobiol.* 40, 288–301.